HAL
open science

All-sky, all-frequency directional search for persistent gravitational waves from Advanced LIGO's and Advanced Virgo's first three observing runs

R. Abbott, T. D. Abbott, F. Acernese, K. Ackley, C. Adams, N. Adhikari, R. X. Adhikari, V. B. Adya, C. Affeldt, D. Agarwal, et al.

To cite this version:

R. Abbott, T. D. Abbott, F. Acernese, K. Ackley, C. Adams, et al.. All-sky, all-frequency directional search for persistent gravitational waves from Advanced LIGO's and Advanced Virgo's first three observing runs. Physical Review D, 2022, 105 (12), pp.122001. 10.1103/PhysRevD.105.122001 . insu-03711636

HAL Id: insu-03711636

https://insu.hal.science/insu-03711636

Submitted on 11 Aug 2022

HAL is a multi-disciplinary open access archive for the deposit and dissemination of scientific research documents, whether they are published or not. The documents may come from teaching and research institutions in France or abroad, or from public or private research centers.

L'archive ouverte pluridisciplinaire **HAL**, est destinée au dépôt et à la diffusion de documents scientifiques de niveau recherche, publiés ou non, émanant des établissements d'enseignement et de recherche français ou étrangers, des laboratoires publics ou privés.

All-sky, all-frequency directional search for persistent gravitational waves from Advanced LIGO's and Advanced Virgo's first three observing runs

R. Abbott *et al.*[*]
(LIGO Scientific Collaboration, the Virgo Collaboration, and the KAGRA Collaboration)

(Received 25 October 2021; revised 22 February 2022; accepted 17 May 2022; published 3 June 2022)

We present the first results from an all-sky all-frequency (ASAF) search for an anisotropic stochastic gravitational-wave background using the data from the first three observing runs of the Advanced LIGO and Advanced Virgo detectors. Upper limit maps on broadband anisotropies of a persistent stochastic background were published for all observing runs of the LIGO-Virgo detectors. However, a broadband analysis is likely to miss narrowband signals as the signal-to-noise ratio of a narrowband signal can be significantly reduced when combined with detector output from other frequencies. Data folding and the computationally efficient analysis pipeline, `PyStoch`, enable us to perform the radiometer map-making at every frequency bin. We perform the search at 3072 `HEALPix` equal area pixels uniformly tiling the sky and in every frequency bin of width $1/32$ Hz in the range 20–1726 Hz, except for bins that are likely to contain instrumental artefacts and hence are notched. We do not find any statistically significant evidence for the existence of narrowband gravitational-wave signals in the analyzed frequency bins. Therefore, we place 95% confidence upper limits on the gravitational-wave strain for each pixel-frequency pair, the limits are in the range $(0.030 - 9.6) \times 10^{-24}$. In addition, we outline a method to identify candidate pixel-frequency pairs that could be followed up by a more sensitive (and potentially computationally expensive) search, e.g., a matched-filtering-based analysis, to look for fainter nearly monochromatic coherent signals. The ASAF analysis is inherently independent of models describing any spectral or spatial distribution of power. We demonstrate that the ASAF results can be appropriately combined over frequencies and sky directions to successfully recover the broadband directional and isotropic results.

DOI: 10.1103/PhysRevD.105.122001

I. INTRODUCTION

A stochastic gravitational-wave background (SGWB) [1,2] can be created by the superposition of a large number of unresolved independent sources [3–23]. Improvements in detector sensitivity suggest that the network of ground-based gravitational-wave (GW) observatories may be able to observe such a background in the coming years. Astrophysical sources in the nearby universe can make the background anisotropic [24–31]. Directional searches were performed [32–36] on data from the Advanced LIGO-Virgo detectors for two different source categories to probe these anisotropies. One search focuses on a persistent SGWB from a collection of pointlike and extended distributions of sources emitting GWs over a broad frequency range [36–40]. The second search looks for narrowband signals from known locations of potentially detectable continuous wave sources [36].

The past analyses, however, had limited prospects of detecting an unknown narrowband anisotropic stochastic background. The broadband searches are not optimized to detect narrowband signals. While the broadband radiometer search [38,41] is capable of coherently adding signals from multiple narrowband sources, noise from thousands of other frequency bins that do not contain any signal can degrade the signal-to-noise ratio. Moreover, it is straightforward to combine results from a narrowband analysis with appropriate frequency-dependent weight factors to derive the broadband results for a variety of spectral shapes including nonpower law predictions in astrophysical [18,19,42] and cosmological [43–45] scenarios. Such efforts can be further extended to allow the spectral shape to vary across the sky, which is expected when multiple anisotropic backgrounds are simultaneously present in the sensitive frequency bands of the detectors. Performing the directional search at all the narrowband frequency bins separately is thus well motivated. Recent developments on data folding [46] and the introduction of a new analysis pipeline `PyStoch` [47], that have made the radiometer analysis hundreds of times faster, opens up the possibility of performing an all-sky directed radiometer search for unknown persistent signals in narrow frequency bins [48,49].

In addition, many unknown galactic and extra-galactic continuous GW sources, primarily from neutron stars [50–60] and exotic scenarios like boson clouds around spinning black holes [61,62], may be detectable with the Advanced

[*]Full author list given at the end of the article.

 © 2022 American Physical Society

LIGO-Virgo detectors. Searching for such signals from neutron stars across the sky using known models is always computationally expensive [63,64]. Since these matched-filtering-based searches depend on the signal model via frequency evolution templates, the chances of detecting an unknown or poorly modeled family of sources (e.g., accreting and/or short-period binary systems) are limited and expanding the parameter space is computationally challenging [51,65]. Also, the probability of detection in such matched-filtering-based searches is reduced substantially in the presence of glitches [66]. The all-sky all-frequency (ASAF) analysis is robust with respect to modeling and able to rapidly identify candidate frequency—sky location pairs, that may warrant following up with more sensitive matched filtering-based searches.

The ASAF results could also be used to look for cross-correlations between SGWB and the electromagnetic sky [67–70], where each narrowband frequency bins may be analysed independently for setting stronger constraints on astrophysical and cosmological models.

In this paper we report the first ASAF upper limits on an unmodeled anisotropic SGWB using data from the first three observing runs (O1 + O2 + O3) of the Advanced LIGO and Advanced Virgo detectors.

II. DATA

To perform the ASAF search, we analyze the data from the first (O1) and second (O2) observing runs of the Advanced LIGO [71] detectors located in Hanford (H) and Livingston (L), and from the third observing runs (O3) of both Advanced LIGO and Advanced Virgo [72] (V). The recorded data have been processed and conditioned in the same way as was done in the latest directional search analysis by the LIGO-Virgo-KAGRA (LVK) collaboration [36,73–75]. To account for non-Gaussian features in the data, we identify and remove segments containing detected GW signals from compact binary coalescences [36,76,77], nonretracted events in the second half of O3 [78], transient hardware injections (simulated signals injected by physically displacing the interferometer mirrors [79]) and segments associated with instrumental artifacts. We then obtain the cross-spectral density (CSD) by combining the short-term Fourier transforms (SFTs) of 192 second data segments from pairs of detectors [80], and the corresponding variances, with a coarse-grained frequency resolution of $\Delta f = 1/32$ Hz [81].

We apply the ASAF analysis in the frequency range 20–1726 Hz as in the past stochastic searches. In addition to the time-domain data quality cuts, we also identify contaminated frequency bins using coherence studies [82]. These frequency bins are mainly associated with known instrumental artifacts (calibration lines, power lines, and their harmonics). We also remove the continuous-wave hardware injections [79] in the final analysis, though we use these for validating the analysis pipeline. Since we produce results for each frequency bin separately, it is important to have a stringent check on the noise contamination for all the individual bins. In the broadband search [36], while all attempts are made to discard frequency bins with noise contamination, to avoid too much loss of sensitivity, notching is relatively less stringent, as noise in a few frequency bins has an insignificant effect on the whole integrated frequency band. We apply a more stringent threshold on the permissible level of nonstationarity in individual frequency bins compared to the broadband search [83]. This choice results in removing approximately 21%, 34.8%, and 28.2% of the frequency bins from O3 data for HL, HV, and LV baselines, respectively, compared to 14.8%, 25.2%, 21.9%, for the nonstringent notching used in the broadband search [36]. After combining the baselines and the three observing runs, the number of completely notched frequencies reduces to 12.5% of the total.

III. ASAF ESTIMATORS

In contrast to the previous stochastic directional analyses, which constrained either broadband integrated anisotropy of the sky or narrowband sources in specific directions, the ASAF analysis attempts to probe anisotropy of the whole sky in each frequency bin. The anisotropies can be characterized in terms of a dimensionless GW energy density parameter $\Omega_{\rm GW}(f,\hat{\mathbf{n}})$ with units sr^{-1}, defined as [36,80,84],

$$\Omega_{\rm GW}(f,\hat{\mathbf{n}}) \equiv \frac{f}{\rho_{\rm c}}\frac{d\rho_{\rm GW}}{df} = \frac{2\pi^2}{3H_0^2} f^3 \mathcal{P}(f,\hat{\mathbf{n}}), \tag{1}$$

where $\rho_{\rm GW}$ is the energy density of incoming GWs from the direction $\hat{\mathbf{n}}$ observed in the frequency range from f to $f + df$, $\rho_{\rm c} = 3c^2H_0^2/8\pi G$ is the critical energy density needed to close the universe, c denotes the speed of light, G is the gravitational constant, and H_0 is the Hubble constant. We are interested in estimating the sky-maps $\mathcal{P}(f,\hat{\mathbf{n}})$ at every frequency, which can be decomposed as,

$$\mathcal{P}(f,\hat{\mathbf{n}}) = \sum_p \mathcal{P}_p(f) e_p(\hat{\mathbf{n}}), \tag{2}$$

in terms of basis functions $e_p(\hat{\mathbf{n}})$. The choice of the basis usually depends on the target source. For extended sources, the spherical harmonic basis $Y_{lm}(\hat{\mathbf{n}})$ is a common choice, while for localized pointlike sources the pixel basis, $e_p(\hat{\mathbf{n}}) = \delta^2(\hat{\mathbf{n}} - \hat{\mathbf{n}}_p)$, where $\hat{\mathbf{n}}_p$ is the direction of pixel number p, is an appropriate choice. Here we perform the ASAF analysis in pixel basis only.

To measure the anisotropy $\mathcal{P}(f,\hat{\mathbf{n}})$, the radiometer search uses the maximum likelihood (ML) estimator [38,85] as the statistic,

$$\hat{\boldsymbol{\mathcal{P}}}(f) = \boldsymbol{\Gamma}(f)^{-1}\mathbf{X}(f), \tag{3}$$

where $\mathbf{X}$ is the *dirty map* [38] and $\mathbf{\Gamma}$ is the Fisher information matrix [85] in the weak signal limit, where in the chosen basis, the signal is much smaller than the standard deviation of the noise in each data segment. The dirty map $\mathbf{X}$ represents the SGWB sky seen through the response matrices of a baseline $\mathcal{I}$ formed by the detectors $\mathcal{I}_1$ and $\mathcal{I}_2$, defined as

$$X_p(f) = \tau\Delta f \mathfrak{Re}\sum_{\mathcal{I},t}\frac{\gamma^{\mathcal{I}*}_{ft,p}C^{\mathcal{I}}(t;f)}{P_{\mathcal{I}_1}(t;f)P_{\mathcal{I}_2}(t;f)}, \tag{4}$$

where τ is the length (duration) of each time segment, $P_{\mathcal{I}_{1,2}}(t;f)$ denotes the one-sided noise power spectral density (PSD) and $C^{\mathcal{I}}(t;f) := (2/\tau)\tilde{s}^*_{\mathcal{I}_1}(t;f)\tilde{s}_{\mathcal{I}_2}(t;f)$ is the CSD, $\tilde{s}_{\mathcal{I}_{1,2}}(t;f)$ are the SFTs of data from the detectors at a time-segment marked by t. In practice, to prevent spectral leakage without loss of data, overlapping Hanning windows are applied to the time series data in each segment, introducing additional normalization factors, which have been accounted for in the analysis [37,41,81,86,87]. Also, the coarse-grained frequency bin size Δf is greater than $1/\tau$, i.e., $\tau\Delta f$ is not unity [82,88]. The overlap reduction function (ORF), $\gamma^{\mathcal{I}}_{ft,p}$, is defined as

$$\gamma^{\mathcal{I}}_{ft,p} := \sum_A F^A_{\mathcal{I}_1}(\hat{\mathbf{n}}_p,t)F^A_{\mathcal{I}_2}(\hat{\mathbf{n}}_p,t)e^{2\pi i f\hat{\mathbf{n}}_p\cdot\mathbf{\Delta x}_{\mathcal{I}}(t)/c}, \tag{5}$$

where $\mathbf{\Delta x}_{\mathcal{I}}(t)$ is the separation vector between the detectors. In the above equation $A = +,\times$ denotes the polarization (note that this analysis assumes statistically equivalent $+$ and $\times$ polarizations). The ORF is necessary to optimally "point" the radiometer [38] to a direction $\hat{\mathbf{n}}_p$ corresponding to the pixel index p by cross-correlating data streams from pairs of detectors with time varying phase delay, along with the sky modulation induced by the antenna pattern functions of the detector ($F^A_{\mathcal{I}_{1,2}}$) [2,80]. The uncertainty in the dirty map measurement is encoded in the Fisher information matrix defined as

$$\Gamma_{pp'}(f) \equiv \frac{\tau\Delta f}{2}\mathfrak{Re}\sum_{\mathcal{I},t}\frac{\gamma^{\mathcal{I}*}_{ft,p}\gamma^{\mathcal{I}}_{ft,p'}}{P_{\mathcal{I}_1}(t;f)P_{\mathcal{I}_2}(t;f)}. \tag{6}$$

Since the estimators are obtained by summing over a large number of $\tau = 192$ second time-segments, the central limit theorem implies that the noise distribution is approximately Gaussian as long as the total observation is longer than a few hours.

Once $X_p(f)$ and $\Gamma_{pp'}(f)$ are calculated using Eqs. (4) and (6) for all the baselines and observing runs, we combine them to obtain the multi-baseline (HLV here onward) dirty map and Fisher information matrix for all the observing runs. From the combined Fisher matrix and dirty map, we can construct the estimator in Eq. (3). The ML estimator $\hat{\mathcal{P}}$ involves inversion of the Fisher matrix $\mathbf{\Gamma}$ which has singular values associated with certain observed modes on the sky where the baselines are insensitive. For point sources, given the current sensitivity of detectors and the pixel resolution used here, correcting for the pixel-to-pixel correlation hardly makes any difference to the analysis [35]. Therefore, to obtain the estimator of narrowband anisotropy and the corresponding signal-to-noise ratio (SNR), instead of inverting the Fisher matrix we divide the dirty map in a given pixel by the corresponding diagonal element of the Fisher matrix. Then the estimator of narrowband anisotropy and its uncertainty are given by,

$$\hat{\mathcal{P}}(f,\hat{\mathbf{n}}) = [\Gamma_{\hat{\mathbf{n}},\hat{\mathbf{n}}}(f)]^{-1}X_{\hat{\mathbf{n}}}, \tag{7}$$

$$\sigma_{\hat{\mathbf{n}}}(f) = [\Gamma_{\hat{\mathbf{n}},\hat{\mathbf{n}}}(f)]^{-1/2}. \tag{8}$$

Now one can write the observed (SNR) as

$$\rho(f,\hat{\mathbf{n}}) = \hat{\mathcal{P}}(f,\hat{\mathbf{n}})/\sigma_{\hat{\mathbf{n}}}(f). \tag{9}$$

In the absence of any signal, $\rho(f,\hat{\mathbf{n}})$ follows a Gaussian distribution (Fig. 1). This formalism is used to perform the ASAF analysis.

IV. DATA FOLDING AND PYSTOCH

Folding [46] makes use of the temporal symmetry in the detector scan pattern to compress the data into a single sidereal day. This reduces the computational cost of the search by a factor equal to the total number of days in the observation run.

`PyStoch` [47] is a fully python-based standalone pipeline for SGWB map-making that takes full advantage of the compressed folded data and symmetries in the detector setup, further improving the efficiency of the search with respect to the previous analysis pipeline. Both folding and `PyStoch` were recently adapted for the broadband directional search in LIGO-Virgo data [36].

Since folding ensures that the data size is fixed (one sidereal day long) and can be loaded entirely in the memory of most computers, `PyStoch` is able to cast the segment-wise radiometer analysis to a matrix multiplication problem incorporating all the time segments together. This allows interchangeable ordering of operations over time and frequency, which is essential for the ASAF analysis, and efficient parallel processing of data. Here we use `HEALPix` [89] resolution of $N_{\rm side} = 16$, which corresponds to the number of pixels $N_{\rm pix} = 12N^2_{\rm side} = 3072$. In principle, one could use a lower (higher) pixel resolution at lower (higher) frequencies. Since the chosen resolution is adequate for the most sensitive frequency band of the baselines, we refrain from introducing further complexities or using higher resolution in the present analysis. With these search

parameters, it took less than an hour per baseline for each dataset to run on a personal computer [90].

V. DETECTION STATISTICS AND OUTLIERS

In order to search for significant outliers, which could indicate the presence of a signal, we first need to determine the noise background. Since it is impossible to directly measure the detector noise in the absence of persistent GW signals, the background is estimated by introducing a constant unphysical *time-shift* [36,82] of ∼1 second between the data streams from a pair of detectors which is much greater than the light travel time between the interferometers. If a signal is not correlated on longer time scales, which is the case for black hole mergers or the stochastic background created by such "popcorn" type events [91], these time-shifts are expected to remove the signal correlation between detectors and the resultant distribution of the detection statistic will then represent the noise background [92]. However, these constant time-shifts do not completely cancel out the types of sources that have longer coherence. For example, if we consider an isolated neutron star emitting GWs at a certain frequency, the constant time-shift analysis will not remove the presence of such a signal; the signal might appear to originate from a different direction or with an unphysical negative SNR. Since the ASAF results could be useful for identifying potential locations and frequencies of previously unknown neutron stars, we apply an alternative method to alleviate this problem.

We estimate the noise background by adding a *random* time-shift to each contiguous slice of data such that the net shift (1–2 second) is always much greater than the physically permissible time delay. In order to validate this prescription, we use continuous hardware injections of isolated pulsars with varying signal strength performed in Advanced LIGO's second (O2) observation run (the hardware injections for O3 were too weak [63] for the ASAF analysis to recover with enough SNR). To generate the background we first apply the random time-shift for the Hanford-Livingston pair and run the entire analysis. These SNRs are plotted in the histogram shown in Fig. 1 along with a Gaussian fit. It is clear that the time-shifted method is successful in removing the effect of the injected signals (the elevated tails of the distribution), leading to a Gaussian noise background. Had the "foreground" distribution—the distribution of SNR without any unphysical time-shifts (zero-lag)—been inside the 2σ error bars around the Gaussian, we would rule out the presence of any outliers with 95% confidence. The presence of some large negative SNR values for zero-lag in Fig. 1 is due to the mismatch between the circular polarization model implicitly assumed in Eq. (5) for a continuous-wave source and the elliptic polarizations simulated by the hardware injections, some of which are nearly linearly polarized. We searched for 9 injections that were in the analyzed frequency range and with source-frame frequency variation less than 1/32 Hz [93]. Among these, 8 were detected as "outliers" and one as a follow-up candidate (the ninth injection is slightly below the detection threshold, but above the threshold for identifying as a follow-up candidate). The maximum dirty map SNRs are plotted in Fig. 1. In some cases, an injection is recovered also in the previous or the next frequency bin due to spectral leakage [87], which appears as multiple circles very close to one vertical line. The recovered locations of the sources match the locations of injections within the diffraction-limited resolution. Note that, as anticipated, the broadband search did not detect any outliers [83].

In order to identify potential candidates for follow-up, we consider the distribution of maximum pixel SNR, $\rho_{\max}(f) \equiv \max_p[\rho(f, \hat{\mathbf{n}}_p)]$. The maximum SNR are shown as a scatter plot in the right panel of Fig. 1. We divide the whole frequency range into 10 Hz bins, over which the sensitivity of the radiometer does not vary significantly. We make a histogram of $\rho_{\max}(f)$ for all the 1/32 Hz frequency bins in each 10 Hz bin, separately for zero-lag and time-shifted analysis. For each 10 Hz bin, we find the $\rho_{\max}(f)$ that corresponds to 99th percentile (1% false alarm rate) of the maximum SNR distribution for time-shifted data and average it over 3 neighboring 10 Hz bins (yellow line in the right panel of Fig. 1). Any $\rho_{\max}(f)$ that is above this threshold in the zero-lag analysis is marked as a candidate for follow-up studies. All hardware injections lie above this threshold curve and qualify for detailed follow-up studies. The "slope" of the maximum SNR distribution in the scatter plot changes because the diffraction-limited resolution is a function of frequency [38,49]. Therefore, at lower frequencies, the number of independent sky patches is smaller and, hence, the pixels are more correlated. The correlation reduces at higher frequencies.

Reassured by the above hardware injection study, we apply the same procedure to obtain the significance of the results from the ASAF search. The distribution of SNR at each frequency and pixel on the sky are shown in the histogram in the bottom left panel of Fig. 1 along with the SNR distributions from the time-shifted run. It is evident from the figure that the distribution of SNRs follow the noise background and in turn is consistent with Gaussian noise within 2σ error bars. Since the number of frequency-pixel pairs is $\sim 10^8$, there is greater than a 5% probability of at least one high SNR (∼6) observation arising purely from noise, as seen in the tails of the distributions. The ASAF analysis thus rules out the existence of any significant outliers in the O1+O2+O3 data.

We nevertheless apply the same procedure described for hardware injections to identify potential candidates that can be followed up by a more sensitive search. We again consider the distribution of maximum SNRs in each 10 Hz frequency bin. These maxima are plotted in the bottom

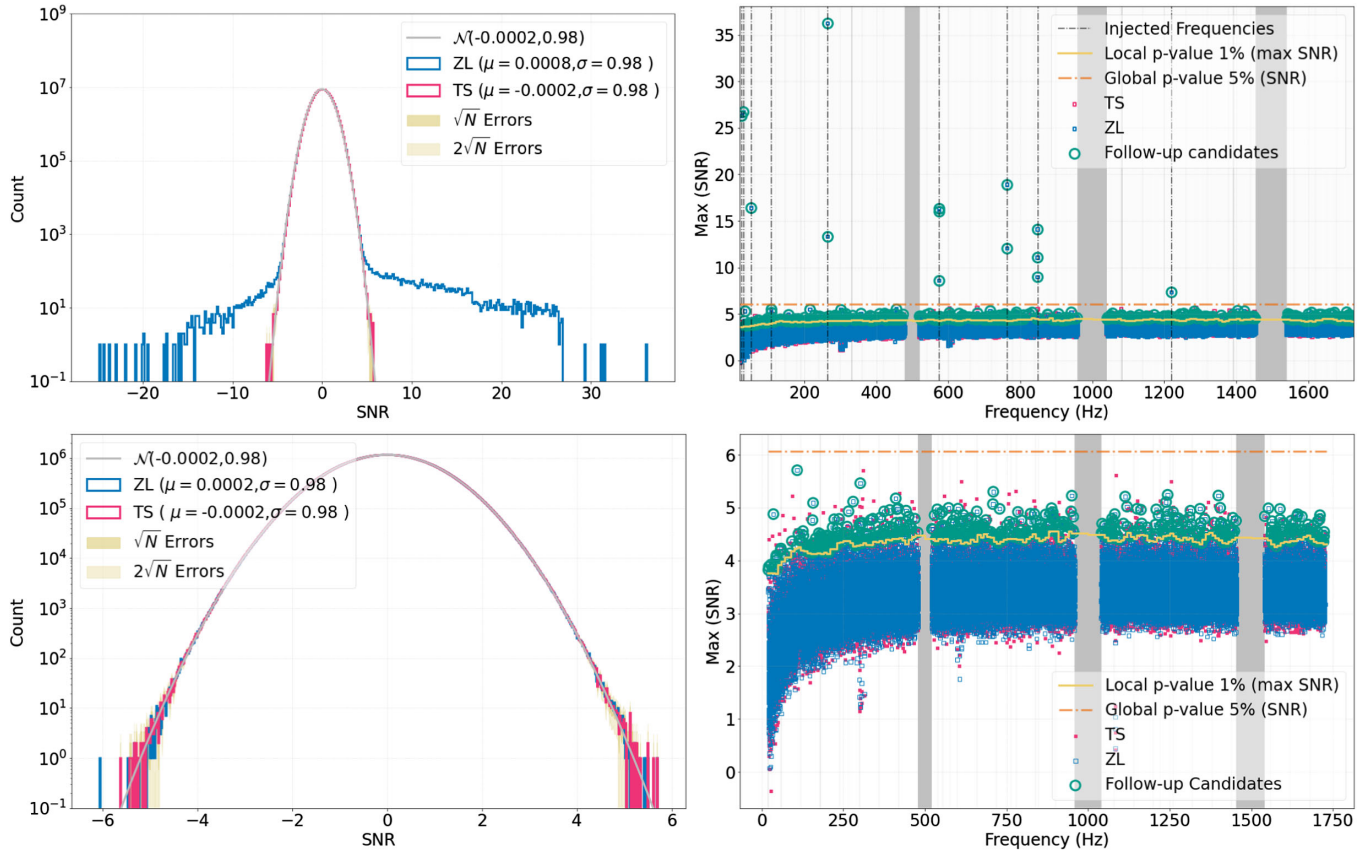

FIG. 1. Results from the O2 hardware injection study (top panel) and O1 + O2 + O3 datasets (bottom panel) are shown. Left hand side plots in the top and bottom panels show the histogram of SNR from both the (unphysical) time-shifted (TS) analysis (red) and zero-lag (ZL) analysis (blue). Time-shifted and zero-lag datasets are both consistent with Gaussian noise (gray histogram) within the 2σ error bars. The outliers cause the extended tails in blue histogram representing the distribution of foreground SNRs. These extended tails in the top left plot depicts the recovery of the hardware injections performed on the O2 data. The point with SNR ~ -6 in bottom left plot is not astrophysically motivated and most likely caused by low number statistics (the two-tailed p-value is more than 5%). The right hand side plots in the top and bottom panels show the distribution of maximum SNRs from both the time-shifted and zero-lag analyses. In these plots, the gray solid vertical lines represent the frequencies notched in the data, the yellow curve shows the 99th percentile of maximum SNR for every 10 Hz frequency bin in the time-shifted analysis, smoothed over 3 neighboring 10 Hz bins, and the orange dot-dashed line delineates the trials-factor-corrected, one-sided global p-value of 5%. The points above the yellow curve, the identified candidates for follow-up studies, are marked with teal circles. For the O2 hardware injection study, one can see that (top right) all the injections are recovered which appear as multiple teal circles very close to the black vertical lines indicating the frequency bin where the injections were made. On the other hand, for O1 + O2 + O3 dataset, we do not find any outliers significantly above the noise background (bottom right). In this case, the teal circles represent 515 candidates which may be followed up by a more sensitive matched-filtering-based analysis.

right panel of Fig. 1. Here, the noise background obtained from the time-shifted method is shown in red in the scatter plot whereas the results from zero-lag data are represented in blue. The yellow line delimits the SNRs above the 99th percentile of the background obtained from the unphysical time-shifted data. The maximum SNRs in the zero-lag analysis that pass this threshold can be classified as candidates for follow-up using template-based searches, even though they are not significant enough to be called outliers by the ASAF analysis—SNR is below the threshold of 6.05 that corresponds to the trials-factor-corrected, one-sided global p-value of 5% shown by the orange dot-dashed line.

VI. UPPER LIMITS

In the presence of a detectable signal of strength $\mathcal{P}(f, \hat{\mathbf{n}})$, the ASAF point estimate, $\hat{\mathcal{P}}(f, \hat{\mathbf{n}})$, by construction would be distributed with a mean $\mathcal{P}(f, \hat{\mathbf{n}})$ and standard deviation $\sigma_{\hat{\mathbf{n}}}(f)$. Since the distribution is found to be consistent with the noise background obtained by unphysical time-shift analysis, ruling out the detection of any significant signal, we set upper limits on the strength of astrophysical signals. Here we take advantage of the fact that this noise background is Gaussian. Since ASAF results are most relevant in the context of nearly monochromatic continuous wave signals, we set Bayesian upper limits on an equivalent strain

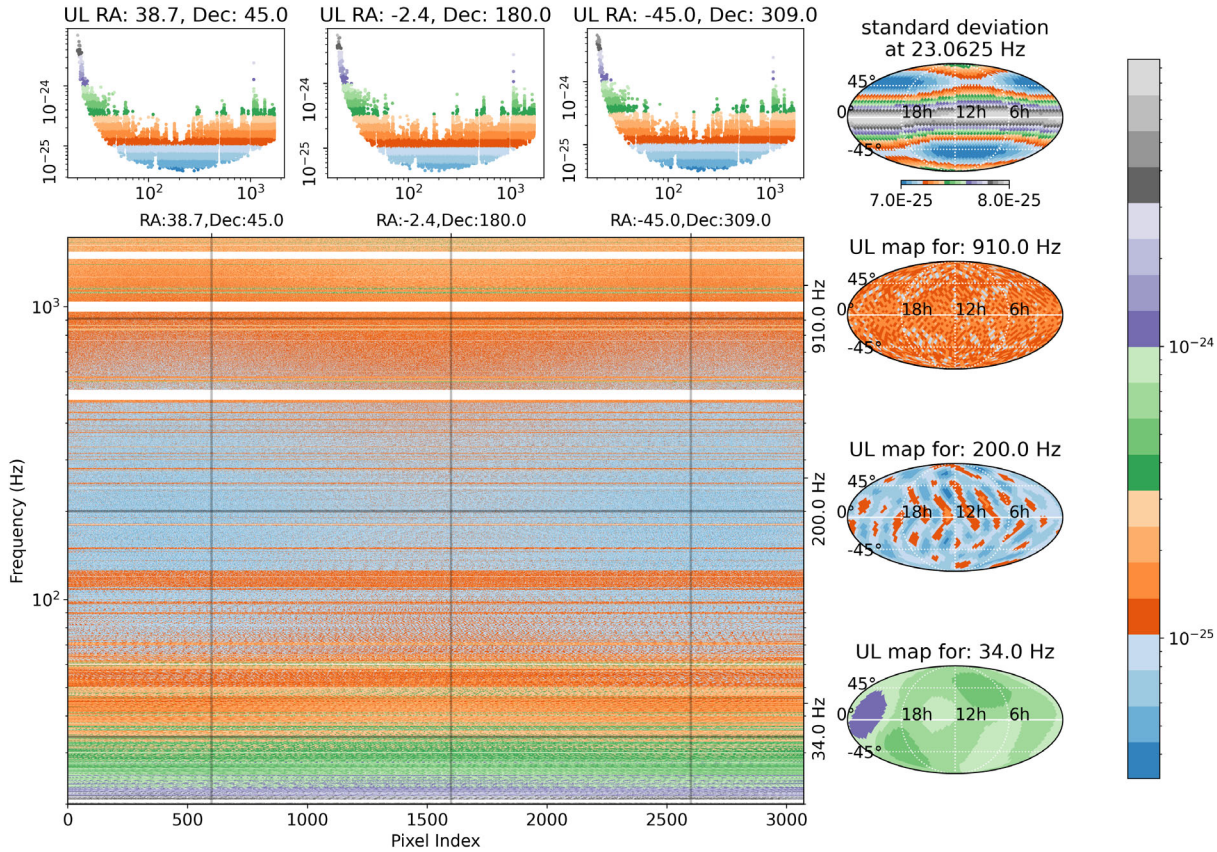

FIG. 2. The 95% confidence Bayesian upper limit on the strain amplitude h for all-sky directions and all-frequency bins. These upper limits are set using the ASAF search performed on the O1 + O2 + O3 dataset. The color bar here denotes the range of upper limit variations. A vertical cross section in this diagram shows the frequency dependent upper limit in a particular direction, 3 such plots are shown in the subplots on top. Whereas horizontal cross sections form a map of upper limits in a particular frequency, 3 such maps are shown on the right. An example of the standard deviation in these maps is also shown in the top right corner.

amplitude of a circularly polarized signal, $h(f,\hat{\mathbf{n}}) = \sqrt{\mathcal{P}(f,\hat{\mathbf{n}})df}$, without correcting for Doppler modulation caused by the Earth's motion. We assume a Gaussian likelihood for $\hat{\mathcal{P}}(f,\hat{\mathbf{n}})$ which is then marginalized over calibration uncertainty [94] with a uniform prior on $h(f,\hat{\mathbf{n}})$ in the wide range $0-10\sigma$ of the point estimate. The 95% confidence Bayesian upper limits placed on the HLV dataset are shown in Fig. 2. The matrix plot shown in Fig. 2 is a qualitative representation of the upper limit, where the upper limit sky maps are plotted as a function of `HEALPix` pixel index on the horizontal axis and frequency on the vertical axis. The color bar represents the respective upper limit range. The horizontal "bands" and gaps in the matrix plot correspond to the notched frequencies in one or more detector pairs. These upper limits are in the range $(0.030\text{–}9.6)\times 10^{-24}$. Note that, when interpreting upper limits on particular frequency-pixel pairs for potential point sources, such as neutron stars, allowance should be made for the angular distance between the source and the center of the pixel containing it; at the highest frequency searched (1726 Hz) the SNR for a point source at the edge of a pixel (at the chosen resolution) is ~20% less than for the same source at the center of the pixel for most parts of the sky. The inclusion of different baselines and observing run data reduces the fraction of completely notched frequencies and also improves the upper limits (more details are provided in [83]). In order to compare the relative sensitivities of different baselines and observing runs, one could define an effective strain sensitivity averaged over all pixels and frequencies (including the notched ones) as $[\langle\sigma_{\hat{\mathbf{n}}}^{-2}(f)\rangle/df^2]^{-1/4}$, which turns out to be 10^{-25} times 1.5, 0.89, 2.5, 2.2, 0.88 and 0.86 respectively, for O1 + O2, HL, LV, HV and HLV for O3 and HLV for O1 + O2 + O3.

We also include the plots of the upper limit sky maps for three example frequencies 34.0 Hz, 200.0 Hz and, 910.0 Hz in Fig. 2. The sky map on the top right corner shows how the uncertainty in the ASAF estimator is nearly axially symmetric and varies in latitude. This pattern is also reflected in the upper limit matrix plot.

VII. DERIVATION OF BROADBAND RADIOMETER (BBR) ESTIMATES FROM ASAF SEARCH

One can integrate the ASAF results over frequency to obtain the broadband radiometer point estimate, variance and upper limits. We invoke the standard assumption used in the BBR search [36], that the anisotropic PSD can be decomposed as a product of frequency and direction dependent terms,

$$\mathcal{P}(f,\hat{\mathbf{n}}) = \mathcal{P}(\hat{\mathbf{n}})H(f), \tag{10}$$

where $H(f)$ is assumed to be a power law model proportional to $(f/f_{\rm ref})^{\alpha}$ where α is the spectral index and $f_{\rm ref}$ is a reference frequency set to 25 Hz. The BBR estimator and its standard deviation [95–97] can then be written in terms of ASAF estimators as

$$\hat{\mathcal{P}}(\hat{\mathbf{n}}) = \frac{\sum_f \hat{\mathcal{P}}(f,\hat{\mathbf{n}})\sigma_{\hat{\mathbf{n}}}^{-2}(f)H(f)}{\sum_f \sigma_{\hat{\mathbf{n}}}^{-2}(f)H^2(f)},$$
$$\sigma_{\hat{\mathbf{n}}} = \left[\sum_f \sigma_{\hat{\mathbf{n}}}^{-2}(f)H^2(f)\right]^{-1/2}. \tag{11}$$

Now one can calculate the GW flux in each direction $\hat{\mathbf{n}}$,

$$\mathcal{F}(\hat{\mathbf{n}}) = \frac{c^3\pi}{4G} f_{\rm ref}^2 \mathcal{P}(\hat{\mathbf{n}}). \tag{12}$$

This quantity has the units of $\mathrm{erg\,cm^{-2}s^{-1}\,Hz^{-1}\,sr^{-1}}$ measured with respect to the reference frequency. Using the methods outlined in [36], we place upper limits on the amount of GW flux in each pixel. The upper limit range obtained from this analysis is reported in Table I. We have also shown in Fig. 3 an example upper limit sky map derived from the ASAF search, performed on the O3 HL folded data for a specific spectral shape ($\alpha = 0$). These limits are consistent with the results we directly obtained from the broadband analysis of O3 data [36].

TABLE I. Broadband directional radiometer upper limit and the isotropic search results derived from the ASAF search (with the stricter notching) using the O3 HL dataset. Results from the previous LVK O3 analyses are also added in the table for a direct comparison. The three spectral indices used in the search are denoted by α.

Broadband results: HL baseline				
α	Upper limit on $\mathcal{F}(\hat{\mathbf{n}})$ $(\times 10^{-8})$		$\hat{\Omega}_{\rm GW,iso}(\times 10^{-9})$	
	ASAF	BBR [36]	ASAF	ISO [82]
0	2.1–9.6	1.8–9.2	2.5 ± 8.6	-2.1 ± 8.2
2/3	1.1–5.6	0.92–4.9	0.61 ± 6.5	-3.4 ± 6.1
3	0.016–0.13	0.014–0.12	-0.49 ± 0.99	-1.3 ± 0.9

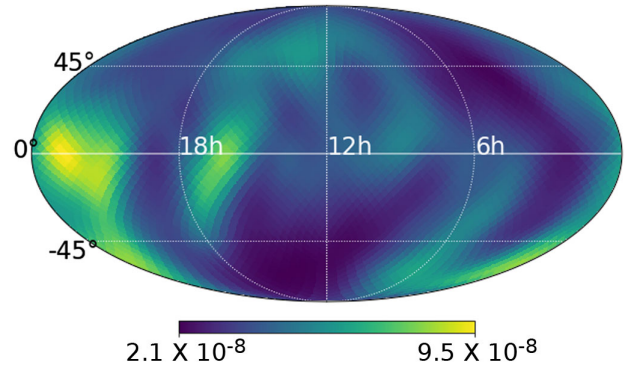

FIG. 3. The broadband 95% confidence GW flux upper limit sky map for $\alpha = 0$ spectral shape. The sky map is represented as a color bar plot on a Mollweide projection of the sky in ecliptic coordinates.

VIII. DERIVATION OF ISOTROPIC ESTIMATES FROM ASAF SEARCH

From the ASAF search, it is also possible to derive the isotropic search results. One can integrate over all the sky directions to obtain the isotropic estimator [98,99].

$$\hat{\mathcal{P}}_{\rm iso}(f)\sigma_{\rm iso}^{-2}(f) = \frac{5}{4\pi}\int d\hat{\mathbf{n}}\,\hat{\mathcal{P}}(f,\hat{\mathbf{n}})\sigma_{\hat{\mathbf{n}}}^{-2}(f),$$
$$\sigma_{\rm iso}^{-2}(f) = \left(\frac{5}{4\pi}\right)^2 \int d\hat{\mathbf{n}} \int d\hat{\mathbf{n}}'\Gamma_{\hat{\mathbf{n}},\hat{\mathbf{n}}'}(f). \tag{13}$$

To compute the standard deviation of the isotropic estimator $\sigma_{\rm iso}(f)$, one requires the full narrowband pixel-to-pixel covariance matrix $\Gamma_{\hat{\mathbf{n}},\hat{\mathbf{n}}'}(f)$ which became computationally realistic with `PyStoch` and folded data. Conventionally isotropic searches report the SGWB in terms of $\Omega_{\rm GW,iso}(f)$. Equation (1) can be used for the corresponding conversion of units. Since the `HEALPix` grid is a discrete grid, we perform discrete integration with $d\hat{\mathbf{n}} = 4\pi/N_{\rm pix}$.

The broadband isotropic estimators can then be derived using Eq. (11) by replacing ASAF estimators with isotropic-all-frequency estimators given in Eq. (13). The cross-correlation spectra from the O3 HL dataset are shown (up to 100 Hz) in Fig. 4 and summarized in Table I. The narrowband uncertainty obtained from the ASAF estimators and the one obtained using the analytically derived isotropic ORF are consistent up to few hundred Hz (which contributes more than 99% sensitivity for the HL baseline [82]). On the other hand, the point estimate and standard deviation of the isotropic broadband estimate shown in Table I differ from our recently published results [36,82] due to different time and frequency domain data quality cuts and a different pixel resolution used in the ASAF analysis.

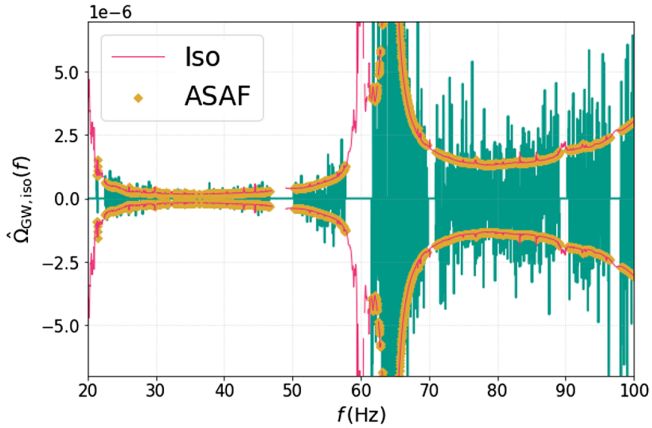

FIG. 4. The isotropic cross-correlation spectra derived from the ASAF analysis using the O3 HL baseline data. The red line depicts the estimated value of standard deviation with the isotropic ORF, while the yellow points show the uncertainty in the cross-power estimator obtained from the ASAF search. The green vertical line, which fluctuates around zero mean represents the point estimates from the ASAF search. The uncertainty calculated from the ASAF maps is not available at certain frequencies due to the more stringent notching.

IX. CONCLUSIONS

We present the first all-sky all-frequency radiometer search results for data from ground-based laser interferometric detectors. No GW signal is detected by our analysis in the first three observing runs from the Advanced LIGO and Advanced Virgo detectors. We set 95% confidence upper limits on the gravitational-wave strain at every frequency bin and sky location searched.

Note that, while the matched-filtering-based analyses can search for neutron stars at narrower frequency bins and are more sensitive [63] when such template-based searches are computationally feasible, ASAF analysis can rapidly search for such monochromatic signals with very little computation power and set upper limits at all frequency and sky-locations for the resolutions used here. The candidate frequency-pixel pairs identified by ASAF can be followed up by matched-filtering-based searches. We employed a heuristic prescription for identifying these follow-up candidates. We recognize that alternative approaches may be explored in this regard. Future analyses will also examine the potential gains from refining frequency and pixel resolution. Since the total number of frequency-pixel pairs is very large ($\sim 10^8$), the prescription must be robust enough not to miss feasibly detectable signals, yet should limit follow-up candidates to a computationally viable number. Also, it may be worth exploring the possibility and effectiveness of incorporating the full ASAF Fisher matrix in the analysis, especially for frequencies below 100 Hz where the pixel correlations may affect the upper limits.

The ASAF maps and Fisher information matrices were also appropriately integrated over frequency, for different choices of spectral models of the background, to recover the previously published search results for the broadband isotropic and anisotropic stochastic backgrounds. The ASAF results could be useful for many other future studies.

ACKNOWLEDGMENTS

This material is based upon work supported by NSF's LIGO Laboratory which is a major facility fully funded by the National Science Foundation. The authors also gratefully acknowledge the support of the Science and Technology Facilities Council (STFC) of the United Kingdom, the Max-Planck-Society (MPS), and the State of Niedersachsen/Germany for support of the construction of Advanced LIGO and construction and operation of the GEO600 detector. Additional support for Advanced LIGO was provided by the Australian Research Council. The authors gratefully acknowledge the Italian Istituto Nazionale di Fisica Nucleare (INFN), the French Centre National de la Recherche Scientifique (CNRS) and the Netherlands Organization for Scientific Research (NWO), for the construction and operation of the Virgo detector and the creation and support of the EGO consortium. The authors also gratefully acknowledge research support from these agencies as well as by the Council of Scientific and Industrial Research of India, the Department of Science and Technology, India, the Science & Engineering Research Board (SERB), India, the Ministry of Human Resource Development, India, the Spanish Agencia Estatal de Investigación (AEI), the Spanish Ministerio de Ciencia e Innovación and Ministerio de Universidades, the Conselleria de Fons Europeus, Universitat i Cultura and the Direcció General de Política Universitaria i Recerca del Govern de les Illes Balears, the Conselleria d'Innovació, Universitats, Ciència i Societat Digital de la Generalitat Valenciana and the CERCA Programme Generalitat de Catalunya, Spain, the National Science Centre of Poland and the European Union—European Regional Development Fund; Foundation for Polish Science (FNP), the Swiss National Science Foundation (SNSF), the Russian Foundation for Basic Research, the Russian Science Foundation, the European Commission, the European Social Funds (ESF), the European Regional Development Funds (ERDF), the Royal Society, the Scottish Funding Council, the Scottish Universities Physics Alliance, the Hungarian Scientific Research Fund (OTKA), the French Lyon Institute of Origins (LIO), the Belgian Fonds de la Recherche Scientifique (FRS-FNRS), Actions de Recherche Concertées (ARC) and Fonds Wetenschappelijk Onderzoek—Vlaanderen (FWO), Belgium, the Paris Île-de-France Region, the National Research, Development and Innovation Office Hungary (NKFIH), the National Research Foundation of Korea, the Natural Science and Engineering Research Council Canada, Canadian Foundation for Innovation (CFI), the Brazilian Ministry of Science, Technology, and Innovations, the

International Center for Theoretical Physics South American Institute for Fundamental Research (ICTP-SAIFR), the Research Grants Council of Hong Kong, the National Natural Science Foundation of China (NSFC), the Leverhulme Trust, the Research Corporation, the Ministry of Science and Technology (MOST), Taiwan, the United States Department of Energy, and the Kavli Foundation. The authors gratefully acknowledge the support of the NSF, STFC, INFN and CNRS for provision of computational resources. This work was supported by MEXT, JSPS Leading-edge Research Infrastructure Program, JSPS Grant-in-Aid for Specially Promoted Research 26000005, JSPS Grant-in-Aid for Scientific Research on Innovative Areas 2905: No. JP17H06358, No. JP17H06361 and No. JP17H06364, JSPS Core-to-Core Program A. Advanced Research Networks, JSPS Grant-in-Aid for Scientific Research (S) No. 17H06133 and No. 20H05639, JSPS Grant-in-Aid for Transformative Research Areas (A) 20A203: No. JP20H05854, the joint research program of the Institute for Cosmic Ray Research, University of Tokyo, National Research Foundation (NRF) and Computing Infrastructure Project of KISTI-GSDC in Korea, Academia Sinica (AS), AS Grid Center (ASGC) and the Ministry of Science and Technology (MoST) in Taiwan under grants including AS-CDA-105-M06, Advanced Technology Center (ATC) of NAOJ, Mechanical Engineering Center of KEK. We would like to thank all of the essential workers who put their health at risk during the COVID-19 pandemic, without whom we would not have been able to complete this work.

[1] Bruce Allen and Adrian C. Ottewill, Detection of anisotropies in the gravitational-wave stochastic background, Phys. Rev. D **56**, 545 (1997).

[2] Joseph D. Romano and Neil J. Cornish, Detection methods for stochastic gravitational-wave backgrounds: A unified treatment, Living Rev. Relativity **20**, 2 (2017).

[3] B. P. Abbott, R. Abbott, T. D. Abbott, F. Acernese, K. Ackley, C. Adams, T. Adams, P. Addesso, R. X. Adhikari, V. B. Adya *et al.*, GW170817: Implications for the Stochastic Gravitational-Wave Background from Compact Binary Coalescences, Phys. Rev. Lett. **120**, 091101 (2018).

[4] Pablo A. Rosado, Gravitational wave background from binary systems, Phys. Rev. D **84**, 084004 (2011).

[5] S. Marassi, R. Schneider, G. Corvino, V. Ferrari, and S. Portegies Zwart, Imprint of the merger and ring-down on the gravitational wave background from black hole binaries coalescence, Phys. Rev. D **84**, 124037 (2011).

[6] Xing-Jiang Zhu, E. Howell, T. Regimbau, D. Blair, and Zong-Hong Zhu, Stochastic gravitational wave background from coalescing binary black holes, Astrophys. J. **739**, 86 (2011).

[7] C. Wu, V. Mandic, and T. Regimbau, Accessibility of the gravitational-wave background due to binary coalescences to second and third generation gravitational-wave detectors, Phys. Rev. D **85**, 104024 (2012).

[8] Xing-Jiang Zhu, Eric J. Howell, David G. Blair, and Zong-Hong Zhu, On the gravitational wave background from compact binary coalescences in the band of ground-based interferometers, Mon. Not. R. Astron. Soc. **431**, 882 (2013).

[9] Irina Dvorkin, Jean-Philippe Uzan, Elisabeth Vangioni, and Joseph Silk, Synthetic model of the gravitational wave background from evolving binary compact objects, Phys. Rev. D **94**, 103011 (2016).

[10] C. Périgois, C. Belczynski, T. Bulik, and T. Regimbau, StarTrack predictions of the stochastic gravitational-wave background from compact binary mergers, Phys. Rev. D **103**, 043002 (2021).

[11] S. Dhurandhar, H. Tagoshi, Y. Okada, N. Kanda, and H. Takahashi, Cross-correlation search for a hot spot of gravitational waves, Phys. Rev. D **84**, 083007 (2011).

[12] Scott A. Hughes, Gravitational wave astronomy and cosmology, Phys. Dark Universe **4**, 86 (2014).

[13] Giulia Cusin, Ruth Durrer, and Pedro G. Ferreira, Polarization of a stochastic gravitational wave background through diffusion by massive structures, Phys. Rev. D **99**, 023534 (2019).

[14] C. M. F. Mingarelli, T. Sidery, I. Mandel, and A. Vecchio, Characterizing gravitational wave stochastic background anisotropy with pulsar timing arrays, Phys. Rev. D **88**, 062005 (2013).

[15] Rennan Bar-Kana, Limits on direct detection of gravitational waves, Phys. Rev. D **50**, 1157 (1994).

[16] Jessica L. Cook and Lorenzo Sorbo, Particle production during inflation and gravitational waves detectable by ground-based interferometers, Phys. Rev. D **85**, 023534 (2012).

[17] S. G. Crowder, R. Namba, V. Mandic, S. Mukohyama, and M. Peloso, Measurement of parity violation in the early universe using gravitational-wave detectors, Phys. Lett. B **726**, 66 (2013).

[18] Tania Regimbau, The astrophysical gravitational wave stochastic background, Res. Astron. Astrophys. **11**, 369 (2011).

[19] Kohei Inayoshi, Kazumi Kashiyama, Eli Visbal, and Zoltan Haiman, Gravitational wave backgrounds from coalescing black hole binaries at cosmic dawn: An upper bound, Astrophys. J. **919**, 41 (2021).

[20] Yuki Watanabe and Eiichiro Komatsu, Improved calculation of the primordial gravitational wave spectrum in the standard model, Phys. Rev. D **73**, 123515 (2006).

[21] Marc Kamionkowski, Arthur Kosowsky, and Michael S. Turner, Gravitational radiation from first-order phase transitions, Phys. Rev. D **49**, 2837 (1994).

[22] Arthur Kosowsky, Michael S. Turner, and Richard Watkins, Gravitational radiation from colliding vacuum bubbles, Phys. Rev. D **45**, 4514 (1992).

[23] Michael S. Turner, Detectability of inflation-produced gravitational waves, Phys. Rev. D **55**, R435 (1997).
[24] Alexander C. Jenkins and Mairi Sakellariadou, Anisotropies in the stochastic gravitational-wave background: Formalism and the cosmic string case, Phys. Rev. D **98**, 063509 (2018).
[25] N. Mazumder, S. Mitra, and S. Dhurandhar, Astrophysical motivation for directed searches for a stochastic gravitational wave background, Phys. Rev. D **89**, 084076 (2014).
[26] Giulia Cusin, Irina Dvorkin, Cyril Pitrou, and Jean-Philippe Uzan, First Predictions of the Angular Power Spectrum of the Astrophysical Gravitational Wave Background, Phys. Rev. Lett. **120**, 231101 (2018).
[27] Alexander C. Jenkins, Mairi Sakellariadou, Tania Regimbau, and Eric Slezak, Anisotropies in the astrophysical gravitational-wave background: Predictions for the detection of compact binaries by LIGO and Virgo, Phys. Rev. D **98**, 063501 (2018).
[28] Pablo A. Rosado, Gravitational wave background from rotating neutron stars, Phys. Rev. D **86**, 104007 (2012).
[29] Cheng-Jian Wu, Vuk Mandic, and Tania Regimbau, Accessibility of the stochastic gravitational wave background from magnetars to the interferometric gravitational wave detectors, Phys. Rev. D **87**, 042002 (2013).
[30] Paul D. Lasky, Mark F. Bennett, and Andrew Melatos, Stochastic gravitational wave background from hydrodynamic turbulence in differentially rotating neutron stars, Phys. Rev. D **87**, 063004 (2013).
[31] Giulia Cusin, Cyril Pitrou, and Jean-Philippe Uzan, Anisotropy of the astrophysical gravitational wave background: Analytic expression of the angular power spectrum and correlation with cosmological observations, Phys. Rev. D **96**, 103019 (2017).
[32] Benjamin P. Abbott *et al.* (LIGO Scientific and Virgo Collaborations), Directional Limits on Persistent Gravitational Waves from Advanced LIGO's First Observing Run, Phys. Rev. Lett. **118**, 121102 (2017).
[33] B. P. Abbott, R. Abbott *et al.* (LIGO Scientific and Virgo Collaborations), Directional limits on persistent gravitational waves using data from advanced LIGO's first two observing runs, Phys. Rev. D **100**, 062001 (2019).
[34] A. I. Renzini and C. R. Contaldi, Improved limits on a stochastic gravitational-wave background and its anisotropies from advanced LIGO O1 and O2 runs, Phys. Rev. D **100**, 063527 (2019).
[35] Deepali Agarwal, Jishnu Suresh, Sanjit Mitra, and Anirban Ain, Upper limits on persistent gravitational waves using folded data and the full covariance matrix from Advanced LIGO's first two observing runs, Phys. Rev. D **104**, 123018 (2021).
[36] R. Abbott *et al.* (LIGO Scientific, Virgo, and KAGRA Collaborations), Search for anisotropic gravitational-wave backgrounds using data from Advanced LIGO's and Advanced Virgo's first three observing runs, Phys. Rev. D **104**, 022005 (2021).
[37] S. W. Ballmer, A radiometer for stochastic gravitational waves, Classical Quantum Gravity **23**, S179 (2006).
[38] Sanjit Mitra, Sanjeev Dhurandhar, Tarun Souradeep, Albert Lazzarini, Vuk Mandic, S. Bose, and S. Ballmer, Gravitational wave radiometry: Mapping a stochastic gravitational wave background, Phys. Rev. D **77**, 042002 (2008).
[39] Eric Thrane, Stefan Ballmer, Joseph D. Romano, Sanjit Mitra, Dipongkar Talukder, Sukanta Bose, and Vuk Mandic, Probing the anisotropies of a stochastic gravitational-wave background using a network of ground-based laser interferometers, Phys. Rev. D **80**, 122002 (2009).
[40] Jishnu Suresh, Anirban Ain, and Sanjit Mitra, Unified mapmaking for an anisotropic stochastic gravitational wave background, Phys. Rev. D **103**, 083024 (2021).
[41] B. Abbott *et al.* (LIGO Scientific and Virgo Collaborations), Upper limit map of a background of gravitational waves, Phys. Rev. D **76**, 082003 (2007).
[42] Stefania Marassi, Raffaella Schneider, and Valeria Ferrari, Gravitational wave backgrounds and the cosmic transition from Population III to Population II stars, Mon. Not. R. Astron. Soc. **398**, 293 (2009).
[43] R. Abbott *et al.* (LIGO Scientific, Virgo, and KAGRA Collaborations), Constraints on Cosmic Strings Using Data from the Third Advanced LIGO–Virgo Observing Run, Phys. Rev. Lett. **126**, 241102 (2021).
[44] Nelson Christensen, Stochastic gravitational wave backgrounds, Rep. Prog. Phys. **82**, 016903 (2019).
[45] Pierre Binetruy, Alejandro Bohe, Chiara Caprini, and Jean-Francois Dufaux, Cosmological backgrounds of gravitational waves and eLISA/NGO: Phase transitions, cosmic strings and other sources, J. Cosmol. Astropart. Phys. 06 (2012) 027.
[46] Anirban Ain, Prathamesh Dalvi, and Sanjit Mitra, Fast gravitational wave radiometry using data folding, Phys. Rev. D **92**, 022003 (2015).
[47] A. Ain, J. Suresh, and S. Mitra, Very fast stochastic gravitational wave background map making using folded data, Phys. Rev. D **98**, 024001 (2018).
[48] Eric Thrane, Sanjit Mitra, Nelson Christensen, Vuk Mandic, and Anirban Ain, All-sky, narrowband, gravitational-wave radiometry with folded data, Phys. Rev. D **91**, 124012 (2015),
[49] Boris Goncharov and Eric Thrane, All-sky radiometer for narrowband gravitational waves using folded data, Phys. Rev. D **98**, 064018 (2018).
[50] Duncan R. Lorimer, Binary and millisecond pulsars, Living Rev. Relativity **11**, 8 (2008).
[51] Keith Riles, Recent searches for continuous gravitational waves, Mod. Phys. Lett. A **32**, 1730035 (2017).
[52] B. P. Abbott *et al.* (LIGO Scientific and Virgo Collaborations), Search for gravitational waves from Scorpius X-1 in the second Advanced LIGO observing run with an improved hidden Markov model, Phys. Rev. D **100**, 122002 (2019).
[53] Yuanhao Zhang, Maria Alessandra Papa, Badri Krishnan, and Anna L. Watts, Search for Continuous Gravitational Waves from Scorpius X-1 in LIGO O2 Data, Astrophys. J. Lett. **906**, L14 (2021).
[54] C. Espinoza, A. Lyne, B. Stappers, and M. Kramer, A study of 315 glitches in the rotation of 102 pulsars, Mon. Not. R. Astron. Soc. **414**, 1679 (2011).
[55] G. Ashton, R. Prix, and D. I. Jones, Statistical characterization of pulsar glitches and their potential impact on searches for continuous gravitational waves, Phys. Rev. D **96**, 063004 (2017).
[56] Sanjeev Dhurandhar, Badri Krishnan, Himan Mukhopadhyay, and John T. Whelan, Cross-correlation

search for periodic gravitational waves, Phys. Rev. D **77**, 082001 (2008).

[57] L. Sun, A. Melatos, P. D. Lasky, C. T. Y. Chung, and N. S. Darman, Cross-correlation search for continuous gravitational waves from a compact object in SNR 1987A in LIGO science run 5, Phys. Rev. D **94**, 082004 (2016).

[58] K. Wette *et al.* (LIGO Scientific Collaboration), Searching for gravitational waves from Cassiopeia A with LIGO, Classical Quantum Gravity **25**, 235011 (2008).

[59] Vladimir Dergachev, Maria Alessandra Papa, Benjamin Steltner, and Heinz-Bernd Eggenstein, Loosely coherent search in LIGO O1 data for continuous gravitational waves from Terzan 5 and the Galactic Center, Phys. Rev. D **99**, 084048 (2019).

[60] Ornella J. Piccinni, P. Astone, S. D'Antonio, S. Frasca, G. Intini, I. La Rosa, P. Leaci, S. Mastrogiovanni, A. Miller, and C. Palomba, Directed search for continuous gravitational-wave signals from the Galactic Center in the Advanced LIGO second observing run, Phys. Rev. D **101**, 082004 (2020).

[61] Richard Brito, Shrobana Ghosh, Enrico Barausse, Emanuele Berti, Vitor Cardoso, Irina Dvorkin, Antoine Klein, and Paolo Pani, Gravitational wave searches for ultralight bosons with LIGO and LISA, Phys. Rev. D **96**, 064050 (2017).

[62] Leo Tsukada, Richard Brito, William E. East, and Nils Siemonsen, Modeling and searching for a stochastic gravitational-wave background from ultralight vector bosons, Phys. Rev. D **103**, 083005 (2021).

[63] R. Abbott *et al.* (LIGO Scientific, VIRGO, and KAGRA Collaborations), All-sky search for continuous gravitational waves from isolated neutron stars in the early O3 LIGO data, Phys. Rev. D **104**, 082004 (2021).

[64] Jing Ming, Maria Alessandra Papa, Heinz-Bernd Eggenstein, Bernd Machenschalk, Benjamin Steltner, Reinhard Prix, Bruce Allen, and Oliver Behnke, Results from an Einstein@Home search for continuous gravitational waves from G347.3 at low frequencies in LIGO O2 data, Astrophys. J. **925**, 8 (2022).

[65] Piotr Jaranowski, Andrzej Królak, and Bernard F. Schutz, Data analysis of gravitational-wave signals from spinning neutron stars: The signal and its detection, Phys. Rev. D **58**, 063001 (1998).

[66] G. Ashton, R. Prix, and D. I. Jones, Statistical characterization of pulsar glitches and their potential impact on searches for continuous gravitational waves, Phys. Rev. D **96**, 063004 (2017).

[67] Suvodip Mukherjee and Joseph Silk, Time-dependence of the astrophysical stochastic gravitational wave background, Mon. Not. R. Astron. Soc. **491**, 4690 (2020).

[68] Kate Ziyan Yang, Vuk Mandic, Claudia Scarlata, and Sharan Banagiri, Searching for cross-correlation between stochastic gravitational wave background and galaxy number counts, Mon. Not. R. Astron. Soc. **500**, 1666 (2020).

[69] Peter Adshead, Niayesh Afshordi, Emanuela Dimastrogiovanni, Matteo Fasiello, Eugene A. Lim, and Gianmassimo Tasinato, Multimessenger cosmology: Correlating cosmic microwave background and stochastic gravitational wave background measurements, Phys. Rev. D **103**, 023532 (2021).

[70] Ameek Malhotra, Ema Dimastrogiovanni, Matteo Fasiello, and Maresuke Shiraishi, Cross-correlations as a diagnostic tool for primordial gravitational waves, J. Cosmol. Astropart. Phys. 03 (2021) 088.

[71] J. Aasi, B. P. Abbott, R. Abbott, T. Abbott, M. R. Abernathy, K. Ackley, C. Adams, T. Adams, P. Addesso *et al.*, Advanced LIGO, Classical Quantum Gravity **32**, 074001 (2015).

[72] F. Acernese, M. Agathos, K. Agatsuma, D. Aisa, N. Allemandou, A. Allocca, J. Amarni, P. Astone, G. Balestri, G. Ballardin *et al.*, Advanced Virgo: A second-generation interferometric gravitational wave detector, Classical Quantum Gravity **32**, 024001 (2015).

[73] E. Goetz, A. Neunzert, K. Riles, A. Matas, S. Kandhasamy, J. Tasson, C. Barschaw, H. Middleton, S. Hughey, L. Mueller, J. Heinzel, J. Carlin, A. Vargas, and I. Hollows (LIGO Scientific and Virgo Collaborations), Unidentified o3 lines found in self-gated c01 data (2021), https://dcc.ligo.org/LIGO-T2100201/public.

[74] K. Riles and J. Zweizig, https://dcc.ligo.org/T2000384/public (2021).

[75] A. Matas, I. Dvorkin, T. Regimbau, and A. Romero, https://dcc.ligo.org/LIGO-P2000546/public (2021).

[76] B. P. Abbott, Richard Abbott, T. D. Abbott, S. Abraham, F. Acernese, K. Ackley, C. Adams, R. X. Adhikari, V. B. Adya, C. Affeldt *et al.* GWTC-1: A Gravitational-Wave Transient Catalog of Compact Binary Mergers Observed by LIGO and Virgo during the First and Second Observing Runs, Phys. Rev. X **9**, 031040 (2019).

[77] R. Abbott *et al.* (LIGO Scientific and Virgo Collaborations), GWTC-2: Compact Binary Coalescences Observed by LIGO and Virgo during the First Half of the Third Observing Run, Phys. Rev. X **11**, 021053 (2021).

[78] https://gracedb.ligo.org/superevents/public/O3/.

[79] C. Biwer *et al.*, Validating gravitational-wave detections: The Advanced LIGO hardware injection system, Phys. Rev. D **95**, 062002 (2017).

[80] B. Allen and J. D. Romano, Detecting a stochastic background of gravitational radiation: Signal processing strategies and sensitivities, Phys. Rev. D **59**, 102001 (1999).

[81] B. P. Abbott *et al.* (LIGO Scientific and Virgo Collaborations), Directional Limits on Persistent Gravitational Waves from Advanced LIGO's First Observing Run, Phys. Rev. Lett. **118**, 121102 (2017).

[82] R. Abbott *et al.* (KAGRA, Virgo, and LIGO Scientific Collaborations), Upper limits on the isotropic gravitational-wave background from Advanced LIGO and Advanced Virgo's third observing run, Phys. Rev. D **104**, 022004 (2021).

[83] Data for All-sky, all-frequency directional search for persistent gravitational-waves from Advanced LIGO's and Advanced Virgo's first three observing runs, https://dcc.ligo.org/LIGO-G2102029/public.

[84] B. Allen, The stochastic gravity-wave background: Sources and detection, in *Relativistic Gravitation and Gravitational Radiation*, edited by J.-A. Marck and J.-P. Lasota, Cambridge Contemporary Astrophysics (Cambridge University Press, Cambridge, England, 1997), pp. 373–417.

[85] E. Thrane, S. Ballmer, J. D. Romano, S. Mitra, D. Talukder, S. Bose, and V. Mandic, Probing the anisotropies of a

stochastic gravitational-wave background using a network of ground-based laser interferometers, Phys. Rev. D **80**, 122002 (2009).

[86] A. Lazzarini and J. Romano, Use of overlapping windows in the stochastic background search, https://dcc.ligo.org/LIGO-T040089/public (2004).

[87] Joseph D. Romano and Neil J. Cornish, Detection methods for stochastic gravitational-wave backgrounds: A unified treatment, Living Rev. Relativity **20**, 2 (2017).

[88] Andrew Matas and Joseph D. Romano, Frequentist versus Bayesian analyses: Cross-correlation as an approximate sufficient statistic for LIGO-Virgo stochastic background searches, Phys. Rev. D **103**, 062003 (2021).

[89] K. M. Gorski, Eric Hivon, A. J. Banday, B. D. Wandelt, F. K. Hansen, M. Reinecke, and M. Bartelman, HEALPix—A framework for high resolution discretization, and fast analysis of data distributed on the sphere, Astrophys. J. **622**, 759 (2005).

[90] An Apple MacBook Pro (2014) laptop with Haswell 2.6 GHz 2-core Intel Core i5 processor (4278U).

[91] Tania Regimbau, The astrophysical gravitational wave stochastic background, Res. Astron. Astrophys. **11**, 369 (2011).

[92] J. Abadie, B. P. Abbott *et al.* (LIGO Scientific and Virgo Collaborations), Directional Limits on Persistent Gravitational Waves Using LIGO S5 Science Data, Phys. Rev. Lett. **107**, 271102 (2011).

[93] https://www.gw-openscience.org/O2_injection_params/.

[94] J. T. Whelan, E. L. Robinson, J. D. Romano, and E. H. Thrane, Treatment of calibration uncertainty in multi-baseline cross-correlation searches for gravitational waves, J. Phys. Conf. Ser. **484**, 012027 (2014).

[95] J. Abadie, B. P. Abbott, R. Abbott *et al.* (LIGO Scientific and Virgo Collaborations), Directional Limits on Persistent Gravitational Waves Using LIGO S5 Science Data, Phys. Rev. Lett. **107**, 271102 (2011).

[96] B. P. Abbott, R. Abbott, T. D. Abbott *et al.* (LIGO Scientific and Virgo Collaborations), Directional Limits on Persistent Gravitational Waves from Advanced LIGO's First Observing Run, Phys. Rev. Lett. **118**, 121102 (2017).

[97] B. P. Abbott, R. Abbott, T. D. Abbott *et al.* (LIGO Scientific and Virgo Collaborations), Directional limits on persistent gravitational waves using data from Advanced LIGO's first two observing runs, Phys. Rev. D **100**, 062001 (2019).

[98] Stefan W. Ballmer, A radiometer for stochastic gravitational waves, Classical Quantum Gravity **23**, S179 (2006).

[99] B. Abbott *et al.* (LIGO Scientific Collaboration), Upper limit map of a background of gravitational waves, Phys. Rev. D **76**, 082003 (2007).

R. Abbott,[1] T. D. Abbott,[2] F. Acernese,[3,4] K. Ackley,[5] C. Adams,[6] N. Adhikari,[7] R. X. Adhikari,[1] V. B. Adya,[8] C. Affeldt,[9,10] D. Agarwal,[11] M. Agathos,[12,13] K. Agatsuma,[14] N. Aggarwal,[15] O. D. Aguiar,[16] L. Aiello,[17] A. Ain,[18] P. Ajith,[19] T. Akutsu,[20,21] S. Albanesi,[22] A. Allocca,[23,4] P. A. Altin,[8] A. Amato,[24] C. Anand,[5] S. Anand,[1] A. Ananyeva,[1] S. B. Anderson,[1] W. G. Anderson,[7] M. Ando,[25,26] T. Andrade,[27] N. Andres,[28] T. Andrić,[29] S. V. Angelova,[30] S. Ansoldi,[31,32] J. M. Antelis,[33] S. Antier,[34] S. Appert,[1] Koji Arai,[1] Koya Arai,[35] Y. Arai,[35] S. Araki,[36] A. Araya,[37] M. C. Araya,[1] J. S. Areeda,[38] M. Arène,[34] N. Aritomi,[25] N. Arnaud,[39,40] S. M. Aronson,[2] K. G. Arun,[41] H. Asada,[42] Y. Asali,[43] G. Ashton,[5] Y. Aso,[44,45] M. Assiduo,[46,47] S. M. Aston,[6] P. Astone,[48] F. Aubin,[28] C. Austin,[2] S. Babak,[34] F. Badaracco,[49] M. K. M. Bader,[50] C. Badger,[51] S. Bae,[52] Y. Bae,[53] A. M. Baer,[54] S. Bagnasco,[22] Y. Bai,[1] L. Baiotti,[55] J. Baird,[34] R. Bajpai,[56] M. Ball,[57] G. Ballardin,[40] S. W. Ballmer,[58] A. Balsamo,[54] G. Baltus,[59] S. Banagiri,[60] D. Bankar,[11] J. C. Barayoga,[1] C. Barbieri,[61,62,63] B. C. Barish,[1] D. Barker,[64] P. Barneo,[27] F. Barone,[65,4] B. Barr,[66] L. Barsotti,[67] M. Barsuglia,[34] D. Barta,[68] J. Bartlett,[64] M. A. Barton,[66,20] I. Bartos,[69] R. Bassiri,[70] A. Basti,[71,18] M. Bawaj,[72,73] J. C. Bayley,[66] A. C. Baylor,[7] M. Bazzan,[74,75] B. Bécsy,[76] V. M. Bedakihale,[77] M. Bejger,[78] I. Belahcene,[39] V. Benedetto,[79] D. Beniwal,[80] T. F. Bennett,[81] J. D. Bentley,[14] M. BenYaala,[30] F. Bergamin,[9,10] B. K. Berger,[70] S. Bernuzzi,[13,66] D. Bersanetti,[82] A. Bertolini,[50] J. Betzwieser,[6] D. Beveridge,[83] R. Bhandare,[84] U. Bhardwaj,[85,50] D. Bhattacharjee,[86] S. Bhaumik,[69] I. A. Bilenko,[87] G. Billingsley,[1] S. Bini,[88,89] R. Birney,[90] O. Birnholtz,[91] S. Biscans,[1,67] M. Bischi,[46,47] S. Biscoveanu,[67] A. Bisht,[9,10] B. Biswas,[11] M. Bitossi,[40,18] M.-A. Bizouard,[92] J. K. Blackburn,[1] C. D. Blair,[83,6] D. G. Blair,[83] R. M. Blair,[64] F. Bobba,[93,94] N. Bode,[9,10] M. Boer,[92] G. Bogaert,[92] M. Boldrini,[95,48] L. D. Bonavena,[74] F. Bondu,[96] E. Bonilla,[70] R. Bonnand,[28] P. Booker,[9,10] B. A. Boom,[50] R. Bork,[1] V. Boschi,[18] N. Bose,[97] S. Bose,[11] V. Bossilkov,[83] V. Boudart,[59] Y. Bouffanais,[74,75] A. Bozzi,[40] C. Bradaschia,[18] P. R. Brady,[7] A. Bramley,[6] A. Branch,[6] M. Branchesi,[29,98] J. E. Brau,[57] M. Breschi,[13] T. Briant,[99] J. H. Briggs,[66] A. Brillet,[92] M. Brinkmann,[9,10] P. Brockill,[7] A. F. Brooks,[1] J. Brooks,[40] D. D. Brown,[80] S. Brunett,[1] G. Bruno,[49] R. Bruntz,[54] J. Bryant,[14] T. Bulik,[100] H. J. Bulten,[50] A. Buonanno,[101,102] R. Buscicchio,[14] D. Buskulic,[28] C. Buy,[103] R. L. Byer,[70] L. Cadonati,[104] G. Cagnoli,[24] C. Cahillane,[64] J. Calderón Bustillo,[105,106] J. D. Callaghan,[66] T. A. Callister,[107,108] E. Calloni,[23,4] J. Cameron,[83] J. B. Camp,[109] M. Canepa,[110,82] S. Canevarolo,[111] M. Cannavacciuolo,[93] K. C. Cannon,[112] H. Cao,[80] Z. Cao,[113] E. Capocasa,[20] E. Capote,[58] G. Carapella,[93,94] F. Carbognani,[40] J. B. Carlin,[114] M. F. Carney,[15] M. Carpinelli,[115,116,40] G. Carrillo,[57] G. Carullo,[71,18] T. L. Carver,[17] J. Casanueva Diaz,[40]

C. Casentini,[117,118] G. Castaldi,[119] S. Caudill,[50,111] M. Cavaglià,[86] F. Cavalier,[39] R. Cavalieri,[40] M. Ceasar,[120] G. Cella,[18] P. Cerdá-Durán,[121] E. Cesarini,[118] W. Chaibi,[92] K. Chakravarti,[11] S. Chalathadka Subrahmanya,[122] E. Champion,[123] C.-H. Chan,[124] C. Chan,[112] C. L. Chan,[106] K. Chan,[106] M. Chan,[125] K. Chandra,[97] P. Chanial,[40] S. Chao,[124] P. Charlton,[126] E. A. Chase,[15] E. Chassande-Mottin,[34] C. Chatterjee,[83] Debarati Chatterjee,[11] Deep Chatterjee,[7] M. Chaturvedi,[84] S. Chaty,[34] C. Chen,[127,128] H. Y. Chen,[67] J. Chen,[124] K. Chen,[129] X. Chen,[83] Y.-B. Chen,[130] Y.-R. Chen,[131] Z. Chen,[17] H. Cheng,[69] C. K. Cheong,[106] H. Y. Cheung,[106] H. Y. Chia,[69] F. Chiadini,[132,94] C-Y. Chiang,[133] G. Chiarini,[75] R. Chierici,[134] A. Chincarini,[82] M. L. Chiofalo,[71,18] A. Chiummo,[40] G. Cho,[135] H. S. Cho,[136] R. K. Choudhary,[83] S. Choudhary,[11] N. Christensen,[92] H. Chu,[129] Q. Chu,[83] Y-K. Chu,[133] S. Chua,[8] K. W. Chung,[51] G. Ciani,[74,75] P. Ciecielag,[78] M. Cieślar,[78] M. Cifaldi,[117,118] A. A. Ciobanu,[80] R. Ciolfi,[137,75] F. Cipriano,[92] A. Cirone,[110,82] F. Clara,[64] E. N. Clark,[138] J. A. Clark,[1,104] L. Clarke,[139] P. Clearwater,[140] S. Clesse,[141] F. Cleva,[92] E. Coccia,[29,98] E. Codazzo,[29] P.-F. Cohadon,[99] D. E. Cohen,[39] L. Cohen,[2] M. Colleoni,[142] C. G. Collette,[143] A. Colombo,[61] M. Colpi,[61,62] C. M. Compton,[64] M. Constancio Jr.,[16] L. Conti,[75] S. J. Cooper,[14] P. Corban,[6] T. R. Corbitt,[2] I. Cordero-Carrión,[144] S. Corezzi,[73,72] K. R. Corley,[43] N. Cornish,[76] D. Corre,[39] A. Corsi,[145] S. Cortese,[40] C. A. Costa,[16] R. Cotesta,[102] M. W. Coughlin,[60] J.-P. Coulon,[92] S. T. Countryman,[43] B. Cousins,[146] P. Couvares,[1] D. M. Coward,[83] M. J. Cowart,[6] D. C. Coyne,[1] R. Coyne,[147] J. D. E. Creighton,[7] T. D. Creighton,[148] A. W. Criswell,[60] M. Croquette,[99] S. G. Crowder,[149] J. R. Cudell,[59] T. J. Cullen,[2] A. Cumming,[66] R. Cummings,[66] L. Cunningham,[66] E. Cuoco,[40,150,18] M. Curyło,[100] P. Dabadie,[24] T. Dal Canton,[39] S. Dall'Osso,[29] G. Dálya,[151] A. Dana,[70] L. M. DaneshgaranBajastani,[81] B. D'Angelo,[110,82] S. Danilishin,[152,50] S. D'Antonio,[118] K. Danzmann,[9,10] C. Darsow-Fromm,[122] A. Dasgupta,[77] L. E. H. Datrier,[66] S. Datta,[11] V. Dattilo,[40] I. Dave,[84] M. Davier,[39] G. S. Davies,[153] D. Davis,[1] M. C. Davis,[120] E. J. Daw,[154] R. Dean,[120] D. DeBra,[70] M. Deenadayalan,[11] J. Degallaix,[155] M. De Laurentis,[23,4] S. Deléglise,[99] V. Del Favero,[123] F. De Lillo,[49] N. De Lillo,[66] W. Del Pozzo,[71,18] L. M. DeMarchi,[15] F. De Matteis,[117,118] V. D'Emilio,[17] N. Demos,[67] T. Dent,[105] A. Depasse,[49] R. De Pietri,[156,157] R. De Rosa,[23,4] C. De Rossi,[40] R. DeSalvo,[119] R. De Simone,[132] S. Dhurandhar,[11] M. C. Díaz,[148] M. Diaz-Ortiz Jr.,[69] N. A. Didio,[58] T. Dietrich,[102,50] L. Di Fiore,[4] C. Di Fronzo,[14] C. Di Giorgio,[93,94] F. Di Giovanni,[121] M. Di Giovanni,[29] T. Di Girolamo,[23,4] A. Di Lieto,[71,18] B. Ding,[143] S. Di Pace,[95,48] I. Di Palma,[95,48] F. Di Renzo,[71,18] A. K. Divakarla,[69] A. Dmitriev,[14] Z. Doctor,[57] L. D'Onofrio,[23,4] F. Donovan,[67] K. L. Dooley,[17] S. Doravari,[11] I. Dorrington,[17] M. Drago,[95,48] J. C. Driggers,[64] Y. Drori,[1] J.-G. Ducoin,[39] P. Dupej,[66] O. Durante,[93,94] D. D'Urso,[115,116] P.-A. Duverne,[39] S. E. Dwyer,[64] C. Eassa,[64] P. J. Easter,[5] M. Ebersold,[158] T. Eckhardt,[122] G. Eddolls,[66] B. Edelman,[57] T. B. Edo,[1] O. Edy,[153] A. Effler,[6] S. Eguchi,[125] J. Eichholz,[8] S. S. Eikenberry,[69] M. Eisenmann,[28] R. A. Eisenstein,[67] A. Ejlli,[17] E. Engelby,[38] Y. Enomoto,[25] L. Errico,[23,4] R. C. Essick,[159] H. Estellés,[142] D. Estevez,[160] Z. Etienne,[161] T. Etzel,[1] M. Evans,[67] T. M. Evans,[6] B. E. Ewing,[146] V. Fafone,[117,118,29] H. Fair,[58] S. Fairhurst,[17] A. M. Farah,[159] S. Farinon,[82] B. Farr,[57] W. M. Farr,[107,108] N. W. Farrow,[5] E. J. Fauchon-Jones,[17] G. Favaro,[74] M. Favata,[162] M. Fays,[59] M. Fazio,[163] J. Feicht,[1] M. M. Fejer,[70] E. Fenyvesi,[68,164] D. L. Ferguson,[165] A. Fernandez-Galiana,[67] I. Ferrante,[71,18] T. A. Ferreira,[16] F. Fidecaro,[71,18] P. Figura,[100] I. Fiori,[40] M. Fishbach,[15] R. P. Fisher,[54] R. Fittipaldi,[166,94] V. Fiumara,[167,94] R. Flaminio,[28,20] E. Floden,[60] H. Fong,[112] J. A. Font,[121,168] B. Fornal,[169] P. W. F. Forsyth,[8] A. Franke,[122] S. Frasca,[95,48] F. Frasconi,[18] C. Frederick,[170] J. P. Freed,[33] Z. Frei,[151] A. Freise,[171] R. Frey,[57] P. Fritschel,[67] V. V. Frolov,[6] G. G. Fronzé,[22] Y. Fujii,[172] Y. Fujikawa,[173] M. Fukunaga,[35] M. Fukushima,[21] P. Fulda,[69] M. Fyffe,[6] H. A. Gabbard,[66] B. U. Gadre,[102] J. R. Gair,[102] J. Gais,[106] S. Galaudage,[5] R. Gamba,[13] D. Ganapathy,[67] A. Ganguly,[19] D. Gao,[174] S. G. Gaonkar,[11] B. Garaventa,[82,110] C. García-Núñez,[90] C. García-Quirós,[142] F. Garufi,[23,4] B. Gateley,[64] S. Gaudio,[33] V. Gayathri,[69] G.-G. Ge,[174] G. Gemme,[82] A. Gennai,[18] J. George,[84] O. Gerberding,[122] L. Gergely,[175] P. Gewecke,[122] S. Ghonge,[104] Abhirup Ghosh,[102] Archisman Ghosh,[176] Shaon Ghosh,[7,162] Shrobana Ghosh,[17] B. Giacomazzo,[61,62,63] L. Giacoppo,[95,48] J. A. Giaime,[2,6] K. D. Giardina,[6] D. R. Gibson,[90] C. Gier,[30] M. Giesler,[177] P. Giri,[18,71] F. Gissi,[79] J. Glanzer,[2] A. E. Gleckl,[38] P. Godwin,[146] E. Goetz,[178] R. Goetz,[69] N. Gohlke,[9,10] B. Goncharov,[5,29] G. González,[2] A. Gopakumar,[179] M. Gosselin,[40] R. Gouaty,[28] D. W. Gould,[8] B. Grace,[8] A. Grado,[180,4] M. Granata,[155] V. Granata,[93] A. Grant,[66] S. Gras,[67] P. Grassia,[1] C. Gray,[64] R. Gray,[66] G. Greco,[72] A. C. Green,[69] R. Green,[17] A. M. Gretarsson,[33] E. M. Gretarsson,[33] D. Griffith,[1] W. Griffiths,[17] H. L. Griggs,[104] G. Grignani,[73,72] A. Grimaldi,[88,89] S. J. Grimm,[29,98] H. Grote,[17] S. Grunewald,[102] P. Gruning,[39] D. Guerra,[121] G. M. Guidi,[46,47] A. R. Guimaraes,[2] G. Guixé,[27] H. K. Gulati,[77] H.-K. Guo,[169] Y. Guo,[50] Anchal Gupta,[1] Anuradha Gupta,[181] P. Gupta,[50,111] E. K. Gustafson,[1] R. Gustafson,[182] F. Guzman,[183] S. Ha,[184] L. Haegel,[34] A. Hagiwara,[35,185] S. Haino,[133] O. Halim,[32,186] E. D. Hall,[67] E. Z. Hamilton,[158] G. Hammond,[66] W.-B. Han,[187] M. Haney,[158] J. Hanks,[64] C. Hanna,[146] M. D. Hannam,[17] O. Hannuksela,[111,50] H. Hansen,[64] T. J. Hansen,[33] J. Hanson,[6] T. Harder,[92] T. Hardwick,[2] K. Haris,[50,111] J. Harms,[29,98] G. M. Harry,[188] I. W. Harry,[153]

D. Hartwig,[122] K. Hasegawa,[35] B. Haskell,[78] R. K. Hasskew,[6] C.-J. Haster,[67] K. Hattori,[189] K. Haughian,[66] H. Hayakawa,[190] K. Hayama,[125] F. J. Hayes,[66] J. Healy,[123] A. Heidmann,[99] A. Heidt,[9,10] M. C. Heintze,[6] J. Heinze,[9,10] J. Heinzel,[191] H. Heitmann,[92] F. Hellman,[192] P. Hello,[39] A. F. Helmling-Cornell,[57] G. Hemming,[40] M. Hendry,[66] I. S. Heng,[66] E. Hennes,[50] J. Hennig,[193] M. H. Hennig,[193] A. G. Hernandez,[81] F. Hernandez Vivanco,[5] M. Heurs,[9,10] S. Hild,[152,50] P. Hill,[30] Y. Himemoto,[194] A. S. Hines,[183] Y. Hiranuma,[195] N. Hirata,[20] E. Hirose,[35] S. Hochheim,[9,10] D. Hofman,[155] J. N. Hohmann,[122] D. G. Holcomb,[120] N. A. Holland,[8] I. J. Hollows,[154] Z. J. Holmes,[80] K. Holt,[6] D. E. Holz,[159] Z. Hong,[196] P. Hopkins,[17] J. Hough,[66] S. Hourihane,[130] E. J. Howell,[83] C. G. Hoy,[17] D. Hoyland,[14] A. Hreibi,[9,10] B-H. Hsieh,[35] Y. Hsu,[124] G-Z. Huang,[196] H-Y. Huang,[133] P. Huang,[174] Y-C. Huang,[131] Y.-J. Huang,[133] Y. Huang,[67] M. T. Hübner,[5] A. D. Huddart,[139] B. Hughey,[33] D. C. Y. Hui,[197] V. Hui,[28] S. Husa,[142] S. H. Huttner,[66] R. Huxford,[146] T. Huynh-Dinh,[6] S. Ide,[198] B. Idzkowski,[100] A. Iess,[117,118] B. Ikenoue,[21] S. Imam,[196] K. Inayoshi,[199] C. Ingram,[80] Y. Inoue,[129] K. Ioka,[200] M. Isi,[67] K. Isleif,[122] K. Ito,[201] Y. Itoh,[202,203] B. R. Iyer,[19] K. Izumi,[204] V. JaberianHamedan,[83] T. Jacqmin,[99] S. J. Jadhav,[205] S. P. Jadhav,[11] A. L. James,[17] A. Z. Jan,[123] K. Jani,[206] J. Janquart,[111,50] K. Janssens,[207,92] N. N. Janthalur,[205] P. Jaranowski,[208] D. Jariwala,[69] R. Jaume,[142] A. C. Jenkins,[51] K. Jenner,[80] C. Jeon,[209] M. Jeunon,[60] W. Jia,[67] H.-B. Jin,[210,211] G. R. Johns,[54] A. W. Jones,[83] D. I. Jones,[212] J. D. Jones,[64] P. Jones,[14] R. Jones,[66] R. J. G. Jonker,[50] L. Ju,[83] P. Jung,[53] k. Jung,[184] J. Junker,[9,10] V. Juste,[160] K. Kaihotsu,[201] T. Kajita,[213] M. Kakizaki,[189] C. V. Kalaghatgi,[17,111] V. Kalogera,[15] B. Kamai,[1] M. Kamiizumi,[190] N. Kanda,[202,203] S. Kandhasamy,[11] G. Kang,[214] J. B. Kanner,[1] Y. Kao,[124] S. J. Kapadia,[19] D. P. Kapasi,[8] S. Karat,[1] C. Karathanasis,[215] S. Karki,[86] R. Kashyap,[146] M. Kasprzack,[1] W. Kastaun,[9,10] S. Katsanevas,[40] E. Katsavounidis,[67] W. Katzman,[6] T. Kaur,[83] K. Kawabe,[64] K. Kawaguchi,[35] N. Kawai,[216] T. Kawasaki,[25] F. Kéfélian,[92] D. Keitel,[142] J. S. Key,[217] S. Khadka,[70] F. Y. Khalili,[87] S. Khan,[17] E. A. Khazanov,[218] N. Khetan,[29,98] M. Khursheed,[84] N. Kijbunchoo,[8] C. Kim,[219] J. C. Kim,[220] J. Kim,[221] K. Kim,[222] W. S. Kim,[223] Y.-M. Kim,[224] C. Kimball,[15] N. Kimura,[185] M. Kinley-Hanlon,[66] R. Kirchhoff,[9,10] J. S. Kissel,[64] N. Kita,[25] H. Kitazawa,[201] L. Kleybolte,[122] S. Klimenko,[69] A. M. Knee,[178] T. D. Knowles,[161] E. Knyazev,[67] P. Koch,[9,10] G. Koekoek,[50,152] Y. Kojima,[225] K. Kokeyama,[226] S. Koley,[29] P. Kolitsidou,[17] M. Kolstein,[215] K. Komori,[67,25] V. Kondrashov,[1] A. K. H. Kong,[227] A. Kontos,[228] N. Koper,[9,10] M. Korobko,[122] K. Kotake,[125] M. Kovalam,[83] D. B. Kozak,[1] C. Kozakai,[44] R. Kozu,[190] V. Kringel,[9,10] N. V. Krishnendu,[9,10] A. Królak,[229,230] G. Kuehn,[9,10] F. Kuei,[124] P. Kuijer,[50] A. Kumar,[205] P. Kumar,[177] Rahul Kumar,[64] Rakesh Kumar,[77] J. Kume,[26] K. Kuns,[67] C. Kuo,[129] H-S. Kuo,[196] Y. Kuromiya,[201] S. Kuroyanagi,[231,232] K. Kusayanagi,[216] S. Kuwahara,[112] K. Kwak,[184] P. Lagabbe,[28] D. Laghi,[71,18] E. Lalande,[233] T. L. Lam,[106] A. Lamberts,[92,234] M. Landry,[64] B. B. Lane,[67] R. N. Lang,[67] J. Lange,[165] B. Lantz,[70] I. La Rosa,[28] A. Lartaux-Vollard,[39] P. D. Lasky,[5] M. Laxen,[6] A. Lazzarini,[1] C. Lazzaro,[74,75] P. Leaci,[95,48] S. Leavey,[9,10] Y. K. Lecoeuche,[178] H. K. Lee,[235] H. M. Lee,[135] H. W. Lee,[220] J. Lee,[135] K. Lee,[236] R. Lee,[131] J. Lehmann,[9,10] A. Lemaître,[237] M. Leonardi,[20] N. Leroy,[39] N. Letendre,[28] C. Levesque,[233] Y. Levin,[5] J. N. Leviton,[182] K. Leyde,[34] A. K. Y. Li,[1] B. Li,[124] J. Li,[15] K. L. Li,[238] T. G. F. Li,[106] X. Li,[130] C-Y. Lin,[239] F-K. Lin,[133] F-L. Lin,[196] H. L. Lin,[129] L. C.-C. Lin,[184] F. Linde,[240,50] S. D. Linker,[81] J. N. Linley,[66] T. B. Littenberg,[241] G. C. Liu,[127] J. Liu,[9,10] K. Liu,[124] X. Liu,[7] F. Llamas,[148] M. Llorens-Monteagudo,[121] R. K. L. Lo,[1] A. Lockwood,[242] L. T. London,[67] A. Longo,[243,244] D. Lopez,[158] M. Lopez Portilla,[111] M. Lorenzini,[117,118] V. Loriette,[245] M. Lormand,[6] G. Losurdo,[18] T. P. Lott,[104] J. D. Lough,[9,10] C. O. Lousto,[123] G. Lovelace,[38] J. F. Lucaccioni,[170] H. Lück,[9,10] D. Lumaca,[117,118] A. P. Lundgren,[153] L.-W. Luo,[133] J. E. Lynam,[54] R. Macas,[153] M. MacInnis,[67] D. M. Macleod,[17] I. A. O. MacMillan,[1] A. Macquet,[92] I. Magaña Hernandez,[7] C. Magazzù,[18] R. M. Magee,[1] R. Maggiore,[14] M. Magnozzi,[82,110] S. Mahesh,[161] E. Majorana,[95,48] C. Makarem,[1] I. Maksimovic,[245] S. Maliakal,[1] A. Malik,[84] N. Man,[92] V. Mandic,[60] V. Mangano,[95,48] J. L. Mango,[246] G. L. Mansell,[64,67] M. Manske,[7] M. Mantovani,[40] M. Mapelli,[74,75] F. Marchesoni,[247,72,248] M. Marchio,[20] F. Marion,[28] Z. Mark,[130] S. Márka,[43] Z. Márka,[43] C. Markakis,[12] A. S. Markosyan,[70] A. Markowitz,[1] E. Maros,[1] A. Marquina,[144] S. Marsat,[34] F. Martelli,[46,47] I. W. Martin,[66] R. M. Martin,[162] M. Martinez,[215] V. A. Martinez,[69] V. Martinez,[24] K. Martinovic,[51] D. V. Martynov,[14] E. J. Marx,[67] H. Masalehdan,[122] K. Mason,[67] E. Massera,[154] A. Masserot,[28] T. J. Massinger,[67] M. Masso-Reid,[66] S. Mastrogiovanni,[34] A. Matas,[102] M. Mateu-Lucena,[142] F. Matichard,[1,67] M. Matiushechkina,[9,10] N. Mavalvala,[67] J. J. McCann,[83] R. McCarthy,[64] D. E. McClelland,[8] P. K. McClincy,[146] S. McCormick,[6] L. McCuller,[67] G. I. McGhee,[66] S. C. McGuire,[249] C. McIsaac,[153] J. McIver,[178] T. McRae,[8] S. T. McWilliams,[161] D. Meacher,[7] M. Mehmet,[9,10] A. K. Mehta,[102] Q. Meijer,[111] A. Melatos,[114] D. A. Melchor,[38] G. Mendell,[64] A. Menendez-Vazquez,[215] C. S. Menoni,[163] R. A. Mercer,[7] L. Mereni,[155] K. Merfeld,[57] E. L. Merilh,[6] J. D. Merritt,[57] M. Merzougui,[92] S. Meshkov,[1,†] C. Messenger,[66] C. Messick,[165] P. M. Meyers,[114] F. Meylahn,[9,10] A. Mhaske,[11] A. Miani,[88,89] H. Miao,[14] I. Michaloliakos,[69] C. Michel,[155] Y. Michimura,[25] H. Middleton,[114] L. Milano,[23] A. L. Miller,[49] A. Miller,[81] B. Miller,[85,50] M. Millhouse,[114] J. C. Mills,[17]

E. Milotti,[186,32] O. Minazzoli,[92,250] Y. Minenkov,[118] N. Mio,[251] Ll. M. Mir,[215] M. Miravet-Tenés,[121] C. Mishra,[252] T. Mishra,[69] T. Mistry,[154] S. Mitra,[11] V. P. Mitrofanov,[87] G. Mitselmakher,[69] R. Mittleman,[67] O. Miyakawa,[190] A. Miyamoto,[202] Y. Miyazaki,[25] K. Miyo,[190] S. Miyoki,[190] Geoffrey Mo,[67] E. Moguel,[170] K. Mogushi,[86] S. R. P. Mohapatra,[67] S. R. Mohite,[7] I. Molina,[38] M. Molina-Ruiz,[192] M. Mondin,[81] M. Montani,[46,47] C. J. Moore,[14] D. Moraru,[64] F. Morawski,[78] A. More,[11] C. Moreno,[33] G. Moreno,[64] Y. Mori,[201] S. Morisaki,[7] Y. Moriwaki,[189] B. Mours,[160] C. M. Mow-Lowry,[14,171] S. Mozzon,[153] F. Muciaccia,[95,48] Arunava Mukherjee,[253] D. Mukherjee,[146] Soma Mukherjee,[148] Subroto Mukherjee,[77] Suvodip Mukherjee,[85] N. Mukund,[9,10] A. Mullavey,[6] J. Munch,[80] E. A. Muñiz,[58] P. G. Murray,[66] R. Musenich,[82,110] S. Muusse,[80] S. L. Nadji,[9,10] K. Nagano,[204] S. Nagano,[254] A. Nagar,[22,255] K. Nakamura,[20] H. Nakano,[256] M. Nakano,[35] R. Nakashima,[216] Y. Nakayama,[201] V. Napolano,[40] I. Nardecchia,[117,118] T. Narikawa,[35] L. Naticchioni,[48] B. Nayak,[81] R. K. Nayak,[257] R. Negishi,[195] B. F. Neil,[83] J. Neilson,[79,94] G. Nelemans,[258] T. J. N. Nelson,[6] M. Nery,[9,10] P. Neubauer,[170] A. Neunzert,[217] K. Y. Ng,[67] S. W. S. Ng,[80] C. Nguyen,[34] P. Nguyen,[57] T. Nguyen,[67] L. Nguyen Quynh,[259] W.-T. Ni,[210,174,131] S. A. Nichols,[2] A. Nishizawa,[26] S. Nissanke,[85,50] E. Nitoglia,[134] F. Nocera,[40] M. Norman,[17] C. North,[17] S. Nozaki,[189] L. K. Nuttall,[153] J. Oberling,[64] B. D. O'Brien,[69] Y. Obuchi,[21] J. O'Dell,[139] E. Oelker,[66] W. Ogaki,[35] G. Oganesyan,[29,98] J. J. Oh,[223] K. Oh,[197] S. H. Oh,[223] M. Ohashi,[190] N. Ohishi,[44] M. Ohkawa,[173] F. Ohme,[9,10] H. Ohta,[112] M. A. Okada,[16] Y. Okutani,[198] K. Okutomi,[190] C. Olivetto,[40] K. Oohara,[195] C. Ooi,[25] R. Oram,[6] B. O'Reilly,[6] R. G. Ormiston,[60] N. D. Ormsby,[54] L. F. Ortega,[69] R. O'Shaughnessy,[123] E. O'Shea,[177] S. Oshino,[190] S. Ossokine,[102] C. Osthelder,[1] S. Otabe,[216] D. J. Ottaway,[80] H. Overmier,[6] A. E. Pace,[146] G. Pagano,[71,18] M. A. Page,[83] G. Pagliaroli,[29,98] A. Pai,[97] S. A. Pai,[84] J. R. Palamos,[57] O. Palashov,[218] C. Palomba,[48] H. Pan,[124] K. Pan,[131,227] P. K. Panda,[205] H. Pang,[129] P. T. H. Pang,[50,111] C. Pankow,[15] F. Pannarale,[95,48] B. C. Pant,[84] F. H. Panther,[83] F. Paoletti,[18] A. Paoli,[40] A. Paolone,[48,260] A. Parisi,[127] H. Park,[7] J. Park,[261] W. Parker,[6,249] D. Pascucci,[50] A. Pasqualetti,[40] R. Passaquieti,[71,18] D. Passuello,[18] M. Patel,[54] M. Pathak,[80] B. Patricelli,[40,18] A. S. Patron,[2] S. Paul,[57] E. Payne,[5] M. Pedraza,[1] M. Pegoraro,[75] A. Pele,[6] F. E. Peña Arellano,[190] S. Penn,[262] A. Perego,[88,89] A. Pereira,[24] T. Pereira,[263] C. J. Perez,[64] C. Périgois,[28] C. C. Perkins,[69] A. Perreca,[88,89] S. Perriès,[134] J. Petermann,[122] D. Petterson,[1] H. P. Pfeiffer,[102] K. A. Pham,[60] K. S. Phukon,[50,240] O. J. Piccinni,[48] M. Pichot,[92] M. Piendibene,[71,18] F. Piergiovanni,[46,47] L. Pierini,[95,48] V. Pierro,[79,94] G. Pillant,[40] M. Pillas,[39] F. Pilo,[18] L. Pinard,[155] I. M. Pinto,[79,94,264] M. Pinto,[40] K. Piotrzkowski,[49] M. Pirello,[64] M. D. Pitkin,[265] E. Placidi,[95,48] L. Planas,[142] W. Plastino,[243,244] C. Pluchar,[138] R. Poggiani,[71,18] E. Polini,[28] D. Y. T. Pong,[106] S. Ponrathnam,[11] P. Popolizio,[40] E. K. Porter,[34] R. Poulton,[40] J. Powell,[140] M. Pracchia,[28] T. Pradier,[160] A. K. Prajapati,[77] K. Prasai,[70] R. Prasanna,[205] G. Pratten,[14] M. Principe,[79,264,94] G. A. Prodi,[266,89] L. Prokhorov,[14] P. Prosposito,[117,118] L. Prudenzi,[102] A. Puecher,[50,111] M. Punturo,[72] F. Puosi,[18,71] P. Puppo,[48] M. Pürrer,[102] H. Qi,[17] V. Quetschke,[148] R. Quitzow-James,[86] F. J. Raab,[64] G. Raaijmakers,[85,50] H. Radkins,[64] N. Radulesco,[92] P. Raffai,[151] S. X. Rail,[233] S. Raja,[84] C. Rajan,[84] K. E. Ramirez,[6] T. D. Ramirez,[38] A. Ramos-Buades,[102] J. Rana,[146] P. Rapagnani,[95,48] U. D. Rapol,[267] A. Ray,[7] V. Raymond,[17] N. Raza,[178] M. Razzano,[71,18] J. Read,[38] L. A. Rees,[188] T. Regimbau,[28] L. Rei,[82] S. Reid,[30] S. W. Reid,[54] D. H. Reitze,[1,69] P. Relton,[17] A. Renzini,[1] P. Rettegno,[268,22] M. Rezac,[38] F. Ricci,[95,48] D. Richards,[139] J. W. Richardson,[1] L. Richardson,[183] G. Riemenschneider,[268,22] K. Riles,[182] S. Rinaldi,[18,71] K. Rink,[178] M. Rizzo,[15] N. A. Robertson,[1,66] R. Robie,[1] F. Robinet,[39] A. Rocchi,[118] S. Rodriguez,[38] L. Rolland,[28] J. G. Rollins,[1] M. Romanelli,[96] J. Romano,[145] R. Romano,[3,4] C. L. Romel,[64] A. Romero-Rodríguez,[215] I. M. Romero-Shaw,[5] J. H. Romie,[6] S. Ronchini,[29,98] L. Rosa,[4,23] C. A. Rose,[7] D. Rosińska,[100] M. P. Ross,[242] S. Rowan,[66] S. J. Rowlinson,[14] S. Roy,[111] Santosh Roy,[11] Soumen Roy,[269] D. Rozza,[115,116] P. Ruggi,[40] K. Ryan,[64] S. Sachdev,[146] T. Sadecki,[64] J. Sadiq,[105] N. Sago,[270] S. Saito,[21] Y. Saito,[190] K. Sakai,[271] Y. Sakai,[195] M. Sakellariadou,[51] Y. Sakuno,[125] O. S. Salafia,[63,62,61] L. Salconi,[40] M. Saleem,[60] F. Salemi,[88,89] A. Samajdar,[50,111] E. J. Sanchez,[1] J. H. Sanchez,[38] L. E. Sanchez,[1] N. Sanchis-Gual,[272] J. R. Sanders,[273] A. Sanuy,[27] T. R. Saravanan,[11] N. Sarin,[5] B. Sassolas,[155] H. Satari,[83] B. S. Sathyaprakash,[146,17] S. Sato,[274] T. Sato,[173] O. Sauter,[69] R. L. Savage,[64] T. Sawada,[202] D. Sawant,[97] H. L. Sawant,[11] S. Sayah,[155] D. Schaetzl,[1] M. Scheel,[130] J. Scheuer,[15] M. Schiworski,[80] P. Schmidt,[14] S. Schmidt,[111] R. Schnabel,[122] M. Schneewind,[9,10] R. M. S. Schofield,[57] A. Schönbeck,[122] B. W. Schulte,[9,10] B. F. Schutz,[17,9,10] E. Schwartz,[17] J. Scott,[66] S. M. Scott,[8] M. Seglar-Arroyo,[28] T. Sekiguchi,[26] Y. Sekiguchi,[275] D. Sellers,[6] A. S. Sengupta,[269] D. Sentenac,[40] E. G. Seo,[106] V. Sequino,[23,4] A. Sergeev,[218] Y. Setyawati,[111] T. Shaffer,[64] M. S. Shahriar,[15] B. Shams,[169] L. Shao,[199] A. Sharma,[29,98] P. Sharma,[84] P. Shawhan,[101] N. S. Shcheblanov,[237] S. Shibagaki,[125] M. Shikauchi,[112] R. Shimizu,[21] T. Shimoda,[25] K. Shimode,[190] H. Shinkai,[276] T. Shishido,[45] A. Shoda,[20] D. H. Shoemaker,[67] D. M. Shoemaker,[165] S. ShyamSundar,[84] M. Sieniawska,[100] D. Sigg,[64] L. P. Singer,[109] D. Singh,[146] N. Singh,[100] A. Singha,[152,50] A. M. Sintes,[142] V. Sipala,[115,116] V. Skliris,[17] B. J. J. Slagmolen,[8] T. J. Slaven-Blair,[83] J. Smetana,[14]

J. R. Smith,[38] R. J. E. Smith,[5] J. Soldateschi,[277,278,47] S. N. Somala,[279] K. Somiya,[216] E. J. Son,[223] K. Soni,[11] S. Soni,[2] V. Sordini,[134] F. Sorrentino,[82] N. Sorrentino,[71,18] H. Sotani,[280] R. Soulard,[92] T. Souradeep,[267,11] E. Sowell,[145] V. Spagnuolo,[152,50] A. P. Spencer,[66] M. Spera,[74,75] R. Srinivasan,[92] A. K. Srivastava,[77] V. Srivastava,[58] K. Staats,[15] C. Stachie,[92] D. A. Steer,[34] J. Steinlechner,[152,50] S. Steinlechner,[152,50] D. J. Stops,[14] M. Stover,[170] K. A. Strain,[66] L. C. Strang,[114] G. Stratta,[281,47] A. Strunk,[64] R. Sturani,[263] A. L. Stuver,[120] S. Sudhagar,[11] V. Sudhir,[67] R. Sugimoto,[282,204] H. G. Suh,[7] T. Z. Summerscales,[283] H. Sun,[83] L. Sun,[8] S. Sunil,[77] A. Sur,[78] J. Suresh,[112,35] P. J. Sutton,[17] Takamasa Suzuki,[173] Toshikazu Suzuki,[35] B. L. Swinkels,[50] M. J. Szczepańczyk,[69] P. Szewczyk,[100] M. Tacca,[50] H. Tagoshi,[35] S. C. Tait,[66] H. Takahashi,[284] R. Takahashi,[20] A. Takamori,[37] S. Takano,[25] H. Takeda,[25] M. Takeda,[202] C. J. Talbot,[30] C. Talbot,[1] H. Tanaka,[285] Kazuyuki Tanaka,[202] Kenta Tanaka,[285] Taiki Tanaka,[35] Takahiro Tanaka,[270] A. J. Tanasijczuk,[49] S. Tanioka,[20,45] D. B. Tanner,[69] D. Tao,[1] L. Tao,[69] E. N. Tapia San Martín,[50,20] C. Taranto,[117] J. D. Tasson,[191] S. Telada,[286] R. Tenorio,[142] J. E. Terhune,[120] L. Terkowski,[122] M. P. Thirugnanasambandam,[11] M. Thomas,[6] P. Thomas,[64] J. E. Thompson,[17] S. R. Thondapu,[84] K. A. Thorne,[6] E. Thrane,[5] Shubhanshu Tiwari,[158] Srishti Tiwari,[11] V. Tiwari,[17] A. M. Toivonen,[60] K. Toland,[66] A. E. Tolley,[153] T. Tomaru,[20] Y. Tomigami,[202] T. Tomura,[190] M. Tonelli,[71,18] A. Torres-Forné,[121] C. I. Torrie,[1] I. Tosta e Melo,[115,116] D. Töyrä,[8] A. Trapananti,[247,72] F. Travasso,[72,247] G. Traylor,[6] M. Trevor,[101] M. C. Tringali,[40] A. Tripathee,[182] L. Troiano,[287,94] A. Trovato,[34] L. Trozzo,[4,190] R. J. Trudeau,[1] D. S. Tsai,[124] D. Tsai,[124] K. W. Tsang,[50,288,111] T. Tsang,[289] J-S. Tsao,[196] M. Tse,[67] R. Tso,[130] K. Tsubono,[25] S. Tsuchida,[202] L. Tsukada,[112] D. Tsuna,[112] T. Tsutsui,[112] T. Tsuzuki,[21] K. Turbang,[290,207] M. Turconi,[92] D. Tuyenbayev,[202] A. S. Ubhi,[14] N. Uchikata,[35] T. Uchiyama,[190] R. P. Udall,[1] A. Ueda,[185] T. Uehara,[291,292] K. Ueno,[112] G. Ueshima,[293] C. S. Unnikrishnan,[179] F. Uraguchi,[21] A. L. Urban,[2] T. Ushiba,[190] A. Utina,[152,50] H. Vahlbruch,[9,10] G. Vajente,[1] A. Vajpeyi,[5] G. Valdes,[183] M. Valentini,[88,89] V. Valsan,[7] N. van Bakel,[50] M. van Beuzekom,[50] J. F. J. van den Brand,[152,294,50] C. Van Den Broeck,[111,50] D. C. Vander-Hyde,[58] L. van der Schaaf,[50] J. V. van Heijningen,[49] J. Vanosky,[1] M. H. P. M. van Putten,[295] N. van Remortel,[207] M. Vardaro,[240,50] A. F. Vargas,[114] V. Varma,[177] M. Vasúth,[68] A. Vecchio,[14] G. Vedovato,[75] J. Veitch,[66] P. J. Veitch,[80] J. Venneberg,[9,10] G. Venugopalan,[1] D. Verkindt,[28] P. Verma,[230] Y. Verma,[84] D. Veske,[43] F. Vetrano,[46] A. Viceré,[46,47] S. Vidyant,[58] A. D. Viets,[246] A. Vijaykumar,[19] V. Villa-Ortega,[105] J.-Y. Vinet,[92] A. Virtuoso,[186,32] S. Vitale,[67] T. Vo,[58] H. Vocca,[73,72] E. R. G. von Reis,[64] J. S. A. von Wrangel,[9,10] C. Vorvick,[64] S. P. Vyatchanin,[87] L. E. Wade,[170] M. Wade,[170] K. J. Wagner,[123] R. C. Walet,[50] M. Walker,[54] G. S. Wallace,[30] L. Wallace,[1] S. Walsh,[7] J. Wang,[174] J. Z. Wang,[182] W. H. Wang,[148] R. L. Ward,[8] J. Warner,[64] M. Was,[28] T. Washimi,[20] N. Y. Washington,[1] J. Watchi,[143] B. Weaver,[64] S. A. Webster,[66] M. Weinert,[9,10] A. J. Weinstein,[1] R. Weiss,[67] C. M. Weller,[242] F. Wellmann,[9,10] L. Wen,[83] P. Weßels,[9,10] K. Wette,[8] J. T. Whelan,[123] D. D. White,[38] B. F. Whiting,[69] C. Whittle,[67] D. Wilken,[9,10] D. Williams,[66] M. J. Williams,[66] A. R. Williamson,[153] J. L. Willis,[1] B. Willke,[9,10] D. J. Wilson,[138] W. Winkler,[9,10] C. C. Wipf,[1] T. Wlodarczyk,[102] G. Woan,[66] J. Woehler,[9,10] J. K. Wofford,[123] I. C. F. Wong,[106] C. Wu,[131] D. S. Wu,[9,10] H. Wu,[131] S. Wu,[131] D. M. Wysocki,[7] L. Xiao,[1] W-R. Xu,[196] T. Yamada,[285] H. Yamamoto,[1] Kazuhiro Yamamoto,[189] Kohei Yamamoto,[285] T. Yamamoto,[190] K. Yamashita,[201] R. Yamazaki,[198] F. W. Yang,[169] L. Yang,[163] Y. Yang,[296] Yang Yang,[69] Z. Yang,[60] M. J. Yap,[8] D. W. Yeeles,[17] A. B. Yelikar,[123] M. Ying,[124] K. Yokogawa,[201] J. Yokoyama,[26,25] T. Yokozawa,[190] J. Yoo,[177] T. Yoshioka,[201] Hang Yu,[130] Haocun Yu,[67] H. Yuzurihara,[35] A. Zadrożny,[230] M. Zanolin,[33] S. Zeidler,[297] T. Zelenova,[40] J.-P. Zendri,[75] M. Zevin,[159] M. Zhan,[174] H. Zhang,[196] J. Zhang,[83] L. Zhang,[1] T. Zhang,[14] Y. Zhang,[183] C. Zhao,[83] G. Zhao,[143] Y. Zhao,[20] Yue Zhao,[169] R. Zhou,[192] Z. Zhou,[15] X. J. Zhu,[5] Z.-H. Zhu,[113] M. E. Zucker,[1,67] and J. Zweizig[1]

(LIGO Scientific Collaboration, the Virgo Collaboration, and the KAGRA Collaboration)

[1]*LIGO Laboratory, California Institute of Technology, Pasadena, California 91125, USA*
[2]*Louisiana State University, Baton Rouge, Louisiana 70803, USA*
[3]*Dipartimento di Farmacia, Università di Salerno, I-84084 Fisciano, Salerno, Italy*
[4]*INFN, Sezione di Napoli, Complesso Universitario di Monte S. Angelo, I-80126 Napoli, Italy*
[5]*OzGrav, School of Physics & Astronomy, Monash University, Clayton 3800, Victoria, Australia*
[6]*LIGO Livingston Observatory, Livingston, Louisiana 70754, USA*
[7]*University of Wisconsin-Milwaukee, Milwaukee, Wisconsin 53201, USA*
[8]*OzGrav, Australian National University, Canberra, Australian Capital Territory 0200, Australia*
[9]*Max Planck Institute for Gravitational Physics (Albert Einstein Institute), D-30167 Hannover, Germany*
[10]*Leibniz Universität Hannover, D-30167 Hannover, Germany*
[11]*Inter-University Centre for Astronomy and Astrophysics, Pune 411007, India*

[12]University of Cambridge, Cambridge CB2 1TN, United Kingdom
[13]Theoretisch-Physikalisches Institut, Friedrich-Schiller-Universität Jena, D-07743 Jena, Germany
[14]University of Birmingham, Birmingham B15 2TT, United Kingdom
[15]Center for Interdisciplinary Exploration & Research in Astrophysics (CIERA), Northwestern University, Evanston, Illinois 60208, USA
[16]Instituto Nacional de Pesquisas Espaciais, 12227-010 São José dos Campos, São Paulo, Brazil
[17]Gravity Exploration Institute, Cardiff University, Cardiff CF24 3AA, United Kingdom
[18]INFN, Sezione di Pisa, I-56127 Pisa, Italy
[19]International Centre for Theoretical Sciences, Tata Institute of Fundamental Research, Bengaluru 560089, India
[20]Gravitational Wave Science Project, National Astronomical Observatory of Japan (NAOJ), Mitaka City, Tokyo 181-8588, Japan
[21]Advanced Technology Center, National Astronomical Observatory of Japan (NAOJ), Mitaka City, Tokyo 181-8588, Japan
[22]INFN Sezione di Torino, I-10125 Torino, Italy
[23]Università di Napoli "Federico II", Complesso Universitario di Monte S. Angelo, I-80126 Napoli, Italy
[24]Université de Lyon, Université Claude Bernard Lyon 1, CNRS, Institut Lumière Matière, F-69622 Villeurbanne, France
[25]Department of Physics, The University of Tokyo, Bunkyo-ku, Tokyo 113-0033, Japan
[26]Research Center for the Early Universe (RESCEU), The University of Tokyo, Bunkyo-ku, Tokyo 113-0033, Japan
[27]Institut de Ciències del Cosmos (ICCUB), Universitat de Barcelona, C/ Martí i Franquès 1, Barcelona, 08028, Spain
[28]Laboratoire d'Annecy de Physique des Particules (LAPP), Univ. Grenoble Alpes, Université Savoie Mont Blanc, CNRS/IN2P3, F-74941 Annecy, France
[29]Gran Sasso Science Institute (GSSI), I-67100 L'Aquila, Italy
[30]SUPA, University of Strathclyde, Glasgow G1 1XQ, United Kingdom
[31]Dipartimento di Scienze Matematiche, Informatiche e Fisiche, Università di Udine, I-33100 Udine, Italy
[32]INFN, Sezione di Trieste, I-34127 Trieste, Italy
[33]Embry-Riddle Aeronautical University, Prescott, Arizona 86301, USA
[34]Université de Paris, CNRS, Astroparticule et Cosmologie, F-75006 Paris, France
[35]Institute for Cosmic Ray Research (ICRR), KAGRA Observatory, The University of Tokyo, Kashiwa City, Chiba 277-8582, Japan
[36]Accelerator Laboratory, High Energy Accelerator Research Organization (KEK), Tsukuba City, Ibaraki 305-0801, Japan
[37]Earthquake Research Institute, The University of Tokyo, Bunkyo-ku, Tokyo 113-0032, Japan
[38]California State University Fullerton, Fullerton, California 92831, USA
[39]Université Paris-Saclay, CNRS/IN2P3, IJCLab, 91405 Orsay, France
[40]European Gravitational Observatory (EGO), I-56021 Cascina, Pisa, Italy
[41]Chennai Mathematical Institute, Chennai 603103, India
[42]Department of Mathematics and Physics, Gravitational Wave Science Project, Hirosaki University, Hirosaki City, Aomori 036-8561, Japan
[43]Columbia University, New York, New York 10027, USA
[44]Kamioka Branch, National Astronomical Observatory of Japan (NAOJ), Kamioka-cho, Hida City, Gifu 506-1205, Japan
[45]The Graduate University for Advanced Studies (SOKENDAI), Mitaka City, Tokyo 181-8588, Japan
[46]Università degli Studi di Urbino "Carlo Bo", I-61029 Urbino, Italy
[47]INFN, Sezione di Firenze, I-50019 Sesto Fiorentino, Firenze, Italy
[48]INFN, Sezione di Roma, I-00185 Roma, Italy
[49]Université catholique de Louvain, B-1348 Louvain-la-Neuve, Belgium
[50]Nikhef, Science Park 105, 1098 XG Amsterdam, Netherlands
[51]King's College London, University of London, London WC2R 2LS, United Kingdom
[52]Korea Institute of Science and Technology Information (KISTI), Yuseong-gu, Daejeon 34141, Republic of Korea
[53]National Institute for Mathematical Sciences, Yuseong-gu, Daejeon 34047, Republic of Korea
[54]Christopher Newport University, Newport News, Virginia 23606, USA
[55]International College, Osaka University, Toyonaka City, Osaka 560-0043, Japan
[56]School of High Energy Accelerator Science, The Graduate University for Advanced Studies (SOKENDAI), Tsukuba City, Ibaraki 305-0801, Japan

[57]University of Oregon, Eugene, Oregon 97403, USA
[58]Syracuse University, Syracuse, New York 13244, USA
[59]Université de Liège, B-4000 Liège, Belgium
[60]University of Minnesota, Minneapolis, Minnesota 55455, USA
[61]Università degli Studi di Milano-Bicocca, I-20126 Milano, Italy
[62]INFN, Sezione di Milano-Bicocca, I-20126 Milano, Italy
[63]INAF, Osservatorio Astronomico di Brera sede di Merate, I-23807 Merate, Lecco, Italy
[64]LIGO Hanford Observatory, Richland, Washington 99352, USA
[65]Dipartimento di Medicina, Chirurgia e Odontoiatria "Scuola Medica Salernitana", Università di Salerno, I-84081 Baronissi, Salerno, Italy
[66]SUPA, University of Glasgow, Glasgow G12 8QQ, United Kingdom
[67]LIGO Laboratory, Massachusetts Institute of Technology, Cambridge, Massachusetts 02139, USA
[68]Wigner RCP, RMKI, H-1121 Budapest, Konkoly Thege Miklós út 29-33, Hungary
[69]University of Florida, Gainesville, Florida 32611, USA
[70]Stanford University, Stanford, California 94305, USA
[71]Università di Pisa, I-56127 Pisa, Italy
[72]INFN, Sezione di Perugia, I-06123 Perugia, Italy
[73]Università di Perugia, I-06123 Perugia, Italy
[74]Università di Padova, Dipartimento di Fisica e Astronomia, I-35131 Padova, Italy
[75]INFN, Sezione di Padova, I-35131 Padova, Italy
[76]Montana State University, Bozeman, Montana 59717, USA
[77]Institute for Plasma Research, Bhat, Gandhinagar 382428, India
[78]Nicolaus Copernicus Astronomical Center, Polish Academy of Sciences, 00-716, Warsaw, Poland
[79]Dipartimento di Ingegneria, Università del Sannio, I-82100 Benevento, Italy
[80]OzGrav, University of Adelaide, Adelaide, South Australia 5005, Australia
[81]California State University, Los Angeles, 5151 State University Dr, Los Angeles, California 90032, USA
[82]INFN, Sezione di Genova, I-16146 Genova, Italy
[83]OzGrav, University of Western Australia, Crawley, Western Australia 6009, Australia
[84]RRCAT, Indore, Madhya Pradesh 452013, India
[85]GRAPPA, Anton Pannekoek Institute for Astronomy and Institute for High-Energy Physics, University of Amsterdam, Science Park 904, 1098 XH Amsterdam, Netherlands
[86]Missouri University of Science and Technology, Rolla, Montana 65409, USA
[87]Faculty of Physics, Lomonosov Moscow State University, Moscow 119991, Russia
[88]Università di Trento, Dipartimento di Fisica, I-38123 Povo, Trento, Italy
[89]INFN, Trento Institute for Fundamental Physics and Applications, I-38123 Povo, Trento, Italy
[90]SUPA, University of the West of Scotland, Paisley PA1 2BE, United Kingdom
[91]Bar-Ilan University, Ramat Gan, 5290002, Israel
[92]Artemis, Université Côte d'Azur, Observatoire de la Côte d'Azur, CNRS, F-06304 Nice, France
[93]Dipartimento di Fisica "E.R. Caianiello", Università di Salerno, I-84084 Fisciano, Salerno, Italy
[94]INFN, Sezione di Napoli, Gruppo Collegato di Salerno, Complesso Universitario di Monte S. Angelo, I-80126 Napoli, Italy
[95]Università di Roma "La Sapienza", I-00185 Roma, Italy
[96]Univ Rennes, CNRS, Institut FOTON—UMR6082, F-3500 Rennes, France
[97]Indian Institute of Technology Bombay, Powai, Mumbai 400 076, India
[98]INFN, Laboratori Nazionali del Gran Sasso, I-67100 Assergi, Italy
[99]Laboratoire Kastler Brossel, Sorbonne Université, CNRS, ENS-Université PSL, Collège de France, F-75005 Paris, France
[100]Astronomical Observatory Warsaw University, 00-478 Warsaw, Poland
[101]University of Maryland, College Park, Maryland 20742, USA
[102]Max Planck Institute for Gravitational Physics (Albert Einstein Institute), D-14476 Potsdam, Germany
[103]L2IT, Laboratoire des 2 Infinis—Toulouse, Université de Toulouse, CNRS/IN2P3, UPS, F-31062 Toulouse Cedex 9, France
[104]School of Physics, Georgia Institute of Technology, Atlanta, Georgia 30332, USA
[105]IGFAE, Campus Sur, Universidade de Santiago de Compostela, 15782 Spain
[106]The Chinese University of Hong Kong, Shatin, NT, Hong Kong
[107]Stony Brook University, Stony Brook, New York 11794, USA
[108]Center for Computational Astrophysics, Flatiron Institute, New York, New York 10010, USA
[109]NASA Goddard Space Flight Center, Greenbelt, Maryland 20771, USA
[110]Dipartimento di Fisica, Università degli Studi di Genova, I-16146 Genova, Italy

[111]Institute for Gravitational and Subatomic Physics (GRASP), Utrecht University, Princetonplein 1, 3584 CC Utrecht, Netherlands
[112]RESCEU, University of Tokyo, Tokyo, 113-0033, Japan
[113]Department of Astronomy, Beijing Normal University, Beijing 100875, China
[114]OzGrav, University of Melbourne, Parkville, Victoria 3010, Australia
[115]Università degli Studi di Sassari, I-07100 Sassari, Italy
[116]INFN, Laboratori Nazionali del Sud, I-95125 Catania, Italy
[117]Università di Roma Tor Vergata, I-00133 Roma, Italy
[118]INFN, Sezione di Roma Tor Vergata, I-00133 Roma, Italy
[119]University of Sannio at Benevento, I-82100 Benevento, Italy and INFN, Sezione di Napoli, I-80100 Napoli, Italy
[120]Villanova University, 800 Lancaster Ave, Villanova, Pennsylvania 19085, USA
[121]Departamento de Astronomía y Astrofísica, Universitat de València, E-46100 Burjassot, València, Spain
[122]Universität Hamburg, D-22761 Hamburg, Germany
[123]Rochester Institute of Technology, Rochester, New York 14623, USA
[124]National Tsing Hua University, Hsinchu City, 30013 Taiwan, Republic of China
[125]Department of Applied Physics, Fukuoka University, Jonan, Fukuoka City, Fukuoka 814-0180, Japan
[126]OzGrav, Charles Sturt University, Wagga Wagga, New South Wales 2678, Australia
[127]Department of Physics, Tamkang University, Danshui Dist., New Taipei City 25137, Taiwan
[128]Department of Physics and Institute of Astronomy, National Tsing Hua University, Hsinchu 30013, Taiwan
[129]Department of Physics, Center for High Energy and High Field Physics, National Central University, Zhongli District, Taoyuan City 32001, Taiwan
[130]CaRT, California Institute of Technology, Pasadena, California 91125, USA
[131]Department of Physics, National Tsing Hua University, Hsinchu 30013, Taiwan
[132]Dipartimento di Ingegneria Industriale (DIIN), Università di Salerno, I-84084 Fisciano, Salerno, Italy
[133]Institute of Physics, Academia Sinica, Nankang, Taipei 11529, Taiwan
[134]Université Lyon, Université Claude Bernard Lyon 1, CNRS, IP2I Lyon / IN2P3, UMR 5822, F-69622 Villeurbanne, France
[135]Seoul National University, Seoul 08826, Republic of Korea
[136]Pusan National University, Busan 46241, Republic of Korea
[137]INAF, Osservatorio Astronomico di Padova, I-35122 Padova, Italy
[138]University of Arizona, Tucson, Arizona 85721, USA
[139]Rutherford Appleton Laboratory, Didcot OX11 0DE, United Kingdom
[140]OzGrav, Swinburne University of Technology, Hawthorn VIC 3122, Australia
[141]Université libre de Bruxelles, Avenue Franklin Roosevelt 50–1050 Bruxelles, Belgium
[142]Universitat de les Illes Balears, IAC3—IEEC, E-07122 Palma de Mallorca, Spain
[143]Université Libre de Bruxelles, Brussels 1050, Belgium
[144]Departamento de Matemáticas, Universitat de València, E-46100 Burjassot, València, Spain
[145]Texas Tech University, Lubbock, Texas 79409, USA
[146]The Pennsylvania State University, University Park, Pennsylvania 16802, USA
[147]University of Rhode Island, Kingston, Rhode Island 02881, USA
[148]The University of Texas Rio Grande Valley, Brownsville, Texas 78520, USA
[149]Bellevue College, Bellevue, Washington 98007, USA
[150]Scuola Normale Superiore, Piazza dei Cavalieri, 7–56126 Pisa, Italy
[151]MTA-ELTE Astrophysics Research Group, Institute of Physics, Eötvös University, Budapest 1117, Hungary
[152]Maastricht University, P.O. Box 616, 6200 MD Maastricht, Netherlands
[153]University of Portsmouth, Portsmouth, PO1 3FX, United Kingdom
[154]The University of Sheffield, Sheffield S10 2TN, United Kingdom
[155]Université Lyon, Université Claude Bernard Lyon 1, CNRS, Laboratoire des Matériaux Avancés (LMA), IP2I Lyon / IN2P3, UMR 5822, F-69622 Villeurbanne, France
[156]Dipartimento di Scienze Matematiche, Fisiche e Informatiche, Università di Parma, I-43124 Parma, Italy
[157]INFN, Sezione di Milano Bicocca, Gruppo Collegato di Parma, I-43124 Parma, Italy
[158]Physik-Institut, University of Zurich, Winterthurerstrasse 190, 8057 Zurich, Switzerland
[159]University of Chicago, Chicago, Illinois 60637, USA
[160]Université de Strasbourg, CNRS, IPHC UMR 7178, F-67000 Strasbourg, France
[161]West Virginia University, Morgantown, West Virginia 26506, USA

[162]Montclair State University, Montclair, New Jersey 07043, USA
[163]Colorado State University, Fort Collins, Colorado 80523, USA
[164]Institute for Nuclear Research, Hungarian Academy of Sciences, Bem t'er 18/c, H-4026 Debrecen, Hungary
[165]Department of Physics, University of Texas, Austin, Texas 78712, USA
[166]CNR-SPIN, c/o Università di Salerno, I-84084 Fisciano, Salerno, Italy
[167]Scuola di Ingegneria, Università della Basilicata, I-85100 Potenza, Italy
[168]Observatori Astronòmic, Universitat de València, E-46980 Paterna, València, Spain
[169]The University of Utah, Salt Lake City, Utah 84112, USA
[170]Kenyon College, Gambier, Ohio 43022, USA
[171]Vrije Universiteit Amsterdam, 1081 HV, Amsterdam, Netherlands
[172]Department of Astronomy, The University of Tokyo, Mitaka City, Tokyo 181-8588, Japan
[173]Faculty of Engineering, Niigata University, Nishi-ku, Niigata City, Niigata 950-2181, Japan
[174]State Key Laboratory of Magnetic Resonance and Atomic and Molecular Physics, Innovation Academy for Precision Measurement Science and Technology (APM), Chinese Academy of Sciences, Xiao Hong Shan, Wuhan 430071, China
[175]University of Szeged, Dóm tér 9, Szeged 6720, Hungary
[176]Universiteit Gent, B-9000 Gent, Belgium
[177]Cornell University, Ithaca, New York 14850, USA
[178]University of British Columbia, Vancouver, British Columbia V6T 1Z4, Canada
[179]Tata Institute of Fundamental Research, Mumbai 400005, India
[180]INAF, Osservatorio Astronomico di Capodimonte, I-80131 Napoli, Italy
[181]The University of Mississippi, University, Mississippi 38677, USA
[182]University of Michigan, Ann Arbor, Michigan 48109, USA
[183]Texas A&M University, College Station, Texas 77843, USA
[184]Department of Physics, Ulsan National Institute of Science and Technology (UNIST), Ulju-gun, Ulsan 44919, Republic of Korea
[185]Applied Research Laboratory, High Energy Accelerator Research Organization (KEK), Tsukuba City, Ibaraki 305-0801, Japan
[186]Dipartimento di Fisica, Università di Trieste, I-34127 Trieste, Italy
[187]Shanghai Astronomical Observatory, Chinese Academy of Sciences, Shanghai 200030, China
[188]American University, Washington, D.C. 20016, USA
[189]Faculty of Science, University of Toyama, Toyama City, Toyama 930-8555, Japan
[190]Institute for Cosmic Ray Research (ICRR), KAGRA Observatory, The University of Tokyo, Kamioka-cho, Hida City, Gifu 506-1205, Japan
[191]Carleton College, Northfield, Minnesota 55057, USA
[192]University of California, Berkeley, California 94720, USA
[193]Maastricht University, 6200 MD, Maastricht, Netherlands
[194]College of Industrial Technology, Nihon University, Narashino City, Chiba 275-8575, Japan
[195]Graduate School of Science and Technology, Niigata University, Nishi-ku, Niigata City, Niigata 950-2181, Japan
[196]Department of Physics, National Taiwan Normal University, sec. IV, Taipei 116, Taiwan
[197]Astronomy & Space Science, Chungnam National University, Yuseong-gu, Daejeon 34134, Republic of Korea, Republic of Korea
[198]Department of Physics and Mathematics, Aoyama Gakuin University, Sagamihara City, Kanagawa 252-5258, Japan
[199]Kavli Institute for Astronomy and Astrophysics, Peking University, Haidian District, Beijing 100871, China
[200]Yukawa Institute for Theoretical Physics (YITP), Kyoto University, Sakyou-ku, Kyoto City, Kyoto 606-8502, Japan
[201]Graduate School of Science and Engineering, University of Toyama, Toyama City, Toyama 930-8555, Japan
[202]Department of Physics, Graduate School of Science, Osaka City University, Sumiyoshi-ku, Osaka City, Osaka 558-8585, Japan
[203]Nambu Yoichiro Institute of Theoretical and Experimental Physics (NITEP), Osaka City University, Sumiyoshi-ku, Osaka City, Osaka 558-8585, Japan
[204]Institute of Space and Astronautical Science (JAXA), Chuo-ku, Sagamihara City, Kanagawa 252-0222, Japan

[205]Directorate of Construction, Services & Estate Management, Mumbai 400094, India
[206]Vanderbilt University, Nashville, Tennessee 37235, USA
[207]Universiteit Antwerpen, Prinsstraat 13, 2000 Antwerpen, Belgium
[208]University of Białystok, 15-424 Białystok, Poland
[209]Department of Physics, Ewha Womans University, Seodaemun-gu, Seoul 03760, Republic of Korea
[210]National Astronomical Observatories, Chinese Academic of Sciences, Chaoyang District, Beijing, China
[211]School of Astronomy and Space Science, University of Chinese Academy of Sciences, Chaoyang District, Beijing, China
[212]University of Southampton, Southampton SO17 1BJ, United Kingdom
[213]Institute for Cosmic Ray Research (ICRR), The University of Tokyo, Kashiwa City, Chiba 277-8582, Japan
[214]Chung-Ang University, Seoul 06974, Republic of Korea
[215]Institut de Física d'Altes Energies (IFAE), Barcelona Institute of Science and Technology, and ICREA, E-08193 Barcelona, Spain
[216]Graduate School of Science, Tokyo Institute of Technology, Meguro-ku, Tokyo 152-8551, Japan
[217]University of Washington Bothell, Bothell, Washington 98011, USA
[218]Institute of Applied Physics, Nizhny Novgorod, 603950, Russia
[219]Ewha Womans University, Seoul 03760, Republic of Korea
[220]Inje University Gimhae, South Gyeongsang 50834, Republic of Korea
[221]Department of Physics, Myongji University, Yongin 17058, Republic of Korea
[222]Korea Astronomy and Space Science Institute, Daejeon 34055, Republic of Korea
[223]National Institute for Mathematical Sciences, Daejeon 34047, Republic of Korea
[224]Ulsan National Institute of Science and Technology, Ulsan 44919, Republic of Korea
[225]Department of Physical Science, Hiroshima University, Higashihiroshima City, Hiroshima 903-0213, Japan
[226]School of Physics and Astronomy, Cardiff University, Cardiff, CF24 3AA, UK
[227]Institute of Astronomy, National Tsing Hua University, Hsinchu 30013, Taiwan
[228]Bard College, 30 Campus Rd, Annandale-On-Hudson, New York 12504, USA
[229]Institute of Mathematics, Polish Academy of Sciences, 00656 Warsaw, Poland
[230]National Center for Nuclear Research, 05-400 Świerk-Otwock, Poland
[231]Instituto de Fisica Teorica, 28049 Madrid, Spain
[232]Department of Physics, Nagoya University, Chikusa-ku, Nagoya, Aichi 464-8602, Japan
[233]Université de Montréal/Polytechnique, Montreal, Quebec H3T 1J4, Canada
[234]Laboratoire Lagrange, Université Côte d'Azur, Observatoire Côte d'Azur, CNRS, F-06304 Nice, France
[235]Department of Physics, Hanyang University, Seoul 04763, Republic of Korea
[236]Sungkyunkwan University, Seoul 03063, Republic of Korea
[237]NAVIER, École des Ponts, Univ Gustave Eiffel, CNRS, Marne-la-Vallée, France
[238]Department of Physics, National Cheng Kung University, Tainan City 701, Taiwan
[239]National Center for High-performance computing, National Applied Research Laboratories, Hsinchu Science Park, Hsinchu City 30076, Taiwan
[240]Institute for High-Energy Physics, University of Amsterdam, Science Park 904, 1098 XH Amsterdam, Netherlands
[241]NASA Marshall Space Flight Center, Huntsville, Alabama 35811, USA
[242]University of Washington, Seattle, Washington 98195, USA
[243]Dipartimento di Matematica e Fisica, Università degli Studi Roma Tre, I-00146 Roma, Italy
[244]INFN, Sezione di Roma Tre, I-00146 Roma, Italy
[245]ESPCI, CNRS, F-75005 Paris, France
[246]Concordia University Wisconsin, Mequon, Wisconsin 53097, USA
[247]Università di Camerino, Dipartimento di Fisica, I-62032 Camerino, Italy
[248]School of Physics Science and Engineering, Tongji University, Shanghai 200092, China
[249]Southern University and A&M College, Baton Rouge, Louisiana 70813, USA
[250]Centre Scientifique de Monaco, 8 quai Antoine Ier, MC-98000, Monaco
[251]Institute for Photon Science and Technology, The University of Tokyo, Bunkyo-ku, Tokyo 113-8656, Japan
[252]Indian Institute of Technology Madras, Chennai 600036, India
[253]Saha Institute of Nuclear Physics, Bidhannagar, West Bengal 700064, India

[254]The Applied Electromagnetic Research Institute, National Institute of Information and Communications Technology (NICT), Koganei City, Tokyo 184-8795, Japan
[255]Institut des Hautes Etudes Scientifiques, F-91440 Bures-sur-Yvette, France
[256]Faculty of Law, Ryukoku University, Fushimi-ku, Kyoto City, Kyoto 612-8577, Japan
[257]Indian Institute of Science Education and Research, Kolkata, Mohanpur, West Bengal 741252, India
[258]Department of Astrophysics/IMAPP, Radboud University Nijmegen, P.O. Box 9010, 6500 GL Nijmegen, Netherlands
[259]Department of Physics, University of Notre Dame, Notre Dame, Indiana 46556, USA
[260]Consiglio Nazionale delle Ricerche—Istituto dei Sistemi Complessi, Piazzale Aldo Moro 5, I-00185 Roma, Italy
[261]Korea Astronomy and Space Science Institute (KASI), Yuseong-gu, Daejeon 34055, Republic of Korea
[262]Hobart and William Smith Colleges, Geneva, New York 14456, USA
[263]International Institute of Physics, Universidade Federal do Rio Grande do Norte, Natal RN 59078-970, Brazil
[264]Museo Storico della Fisica e Centro Studi e Ricerche "Enrico Fermi", I-00184 Roma, Italy
[265]Lancaster University, Lancaster LA1 4YW, United Kingdom
[266]Università di Trento, Dipartimento di Matematica, I-38123 Povo, Trento, Italy
[267]Indian Institute of Science Education and Research, Pune, Maharashtra 411008, India
[268]Dipartimento di Fisica, Università degli Studi di Torino, I-10125 Torino, Italy
[269]Indian Institute of Technology, Palaj, Gandhinagar, Gujarat 382355, India
[270]Department of Physics, Kyoto University, Sakyou-ku, Kyoto City, Kyoto 606-8502, Japan
[271]Department of Electronic Control Engineering, National Institute of Technology, Nagaoka College, Nagaoka City, Niigata 940-8532, Japan
[272]Departamento de Matemática da Universidade de Aveiro and Centre for Research and Development in Mathematics and Applications, Campus de Santiago, 3810-183 Aveiro, Portugal
[273]Marquette University, 11420 W. Clybourn St., Milwaukee, Wisconsin 53233, USA
[274]Graduate School of Science and Engineering, Hosei University, Koganei City, Tokyo 184-8584, Japan
[275]Faculty of Science, Toho University, Funabashi City, Chiba 274-8510, Japan
[276]Faculty of Information Science and Technology, Osaka Institute of Technology, Hirakata City, Osaka 573-0196, Japan
[277]Università di Firenze, Sesto Fiorentino I-50019, Italy
[278]INAF, Osservatorio Astrofisico di Arcetri, Largo E. Fermi 5, I-50125 Firenze, Italy
[279]Indian Institute of Technology Hyderabad, Sangareddy, Khandi, Telangana 502285, India
[280]iTHEMS (Interdisciplinary Theoretical and Mathematical Sciences Program), The Institute of Physical and Chemical Research (RIKEN), Wako, Saitama 351-0198, Japan
[281]INAF, Osservatorio di Astrofisica e Scienza dello Spazio, I-40129 Bologna, Italy
[282]Department of Space and Astronautical Science, The Graduate University for Advanced Studies (SOKENDAI), Sagamihara City, Kanagawa 252-5210, Japan
[283]Andrews University, Berrien Springs, Michigan 49104, USA
[284]Research Center for Space Science, Advanced Research Laboratories, Tokyo City University, Setagaya, Tokyo 158-0082, Japan
[285]Institute for Cosmic Ray Research (ICRR), Research Center for Cosmic Neutrinos (RCCN), The University of Tokyo, Kashiwa City, Chiba 277-8582, Japan
[286]National Metrology Institute of Japan, National Institute of Advanced Industrial Science and Technology, Tsukuba City, Ibaraki 305-8568, Japan
[287]Dipartimento di Scienze Aziendali—Management and Innovation Systems (DISA-MIS), Università di Salerno, I-84084 Fisciano, Salerno, Italy
[288]Van Swinderen Institute for Particle Physics and Gravity, University of Groningen, Nijenborgh 4, 9747 AG Groningen, Netherlands
[289]Faculty of Science, Department of Physics, The Chinese University of Hong Kong, Shatin, N.T., Hong Kong
[290]Vrije Universiteit Brussel, Boulevard de la Plaine 2, 1050 Ixelles, Belgium
[291]Department of Communications Engineering, National Defense Academy of Japan, Yokosuka City, Kanagawa 239-8686, Japan
[292]Department of Physics, University of Florida, Gainesville, Florida 32611, USA
[293]Department of Information and Management Systems Engineering, Nagaoka University of Technology, Nagaoka City, Niigata 940-2188, Japan
[294]Vrije Universiteit Amsterdam, 1081 HV Amsterdam, Netherlands

[295]*Department of Physics and Astronomy, Sejong University, Gwangjin-gu, Seoul 143-747, Republic of Korea*
[296]*Department of Electrophysics, National Chiao Tung University, Hsinchu, Taiwan*
[297]*Department of Physics, Rikkyo University, Toshima-ku, Tokyo 171-8501, Japan*

[†]Deceased.